NOAA Technical Memorandum
NESDIS AISC 13

Assessment of Crop Conditions in Africa

Douglas M. Le Comte
Felix N. Kogan
Carla A. Steinborn
Larason Lambert

Washington, D.C.
January 1988

UNITED STATES
DEPARTMENT OF COMMERCE

National Oceanic and
Atmospheric Administration

National Environmental Satellite
Data and Information Service

NOAA TECHNICAL MEMORANDA

...vironmental Satellite, Data, and Information Service,
...sment and Information Services Center Subseries

...nt and Information Services Center (AISC) provides
...sis of environmental information to support national needs and goals. The products and services of AISC's staff of environmental scientists, meteorologists, and information and computer specialists provide decision assistance to the nation's resource managers. AISC's programs in environmental data analysis and environmental information management complement the data collection and archival program of other National Environmental Satellite, Data, and Information Service (NESDIS) components.

The Technical Memorandum series provides an informal medium for the documentation and quick dissemination of results not appropriate, or not yet ready, for formal publication in the standard journals. The series is used to report on work in progress, to describe technical procedures and practices, or to report to a limited audience.

These papers are available from the originating office and also from the National Technical Information Service (NTIS), U.S. Department of Commerce, 5285 Port Royal Road, Springfield, VA 22151. Prices vary for paper copy and microfiche.

NESDIS Technical Memoranda

AISC 1 Assessment Models for Surface Dispersion of Marine Pollutants. Kurt W. Hess, Fred G. Everdale, and Peter L. Grose, May 1985.

AISC 2 Comparison of Boundary Layer Winds from NWS LFM Output and Instrumented Buoys. Robert W. Reeves and Peter J. Pytlowany, May 1985.

AISC 3 Assessments Model for Estuarine Circulation and Salinity. Kurt W. Hess, June 1985.

AISC 4 Development of a Tropical Cyclone Damage Assessment Methodology. Isobel C. Sheifer and John O. Ellis, January 1986.

AISC 5 Interdisciplinary Synoptic Assessment of Chesapeake Bay and the Adjacent Shelf. Edited by David F. Johnson, Kurt W. Hess, and Peter J. Pytlowany, August 1986.

AISC 6 Numerical Model of Circulation in Chesapeake Bay and the Continental Shelf. Kurt W. Hess, November 1986.

AISC 7 Application of AVHRR Satellite Data to the Study of Sediment and Chlorophyll in Turbid Coastal Water. Richard P. Stumpf, March 1987.

(Continued on inside back cover)

NOAA Technical Memorandum NESDIS AISC 13

Assessment of Crop Conditions in Africa

Douglas M. Le Comte
Felix N. Kogan
Carla A. Steinborn
Larason Lambert

Climate Impact Assessment Division
Assessment and Information Services Center

Washington, D.C.
January 1988

UNITED STATES DEPARTMENT OF COMMERCE
C. William Verity
Secretary

National Oceanic and Atmospheric Administration
J. Curtis Mack, II
Acting Under Secretary

National Environmental Satellite Data and Information Service
Thomas N. Pyke, Jr.
Assistant Administrator

TABLE OF CONTENTS

LIST OF FIGURES

LIST OF TABLES

ABBREVIATIONS AND ACRONYMS

ACCS	Ambroziak Color-Coordinate System
ACORN	area, country, region
AISC	Assessment and Information Services Center
APT	Automatic Picture Transmission
ARC	AGRHYMET Regional Center
AVHRR	Advanced Very High Resolution Radiometer
B	blue (when used in connection with ACCS)
C	cyan (when used in connection with ACCS)
CAB	Climate Assessment Branch of CIAD
CAC	Climate Analysis Center
CARES	Comprehensive Area Rainfall Estimation System
CH_1	Channel 1
CH_2	Channel 2
CIAD	Climate Impact Assessment Division
cm	centimeter
Comp	computed
DCS	Data Collection System
DEC	decadal
EMR	electromagnetic radiation
Eq	equation
FAO	Food and Agriculture Organization
G	green (when used in connection with ACCS)
GAC	Global Area Coverage
GTS	Global Telecommunications System
GVI	Global Vegetation Index
h	hour
ha	hectare
HRPT	High Resolution Picture Transmission
I	intensity
IHS	intensity hue saturation
IMIN	minimum intensity
IR	infrared
ITF	Intertropical Front
kg	kilogram
km	kilometer
LAC	Local Area Coverage
LAI	Leaf Area Index
M	magenta (when used in connection with ACCS)
m	meter
MB	Models Branch of CIAD
mm	millimeter
mt	metric ton
NDVI	Normalized Difference Vegetation Index
NESDIS	National Environmental Satellite, Data, and Information Service
NOAA	National Oceanic and Atmospheric Administration
NTIS	National Technical Information Service
NVI	Normalized Vegetation Index
NWS	National Weather Service
Obs	observed
PCIP	Personal Computer Image Processor
PCP	precipitation

PET	Potential Evapotranspiration
Prcp	precipitation
Qual	quality
R	correlation coefficient
R	red (when used in connection with ACCS)
RGB	red green blue
S	saturation
Sat	satellite
SEM	Space Environmental Monitor Service
SMAX	maximum saturation
SMIN	minimum saturation
STN	station
TECH	technique
Temp	temperature
Tmp	temperature
TOVS	Tiros Operational Vertical Sounder
USAID	United States Agency for International Development
VEG	vegetation
VLF	very low frequency
WMO	World Meterological Organization
WT	weight
Y	yellow (when used in connection with ACCS)
°C	degrees Centigrade
°K	degrees Kelvin
μm	micrometer

ACKNOWLEDGMENTS

Thanks go to the Climate Impact Assessment Division (CIAD) Models Branch (now the Climatic Applications Branch within the NOAA/NESDIS Office of Research and Applications) in Columbia, Missouri. Their material formed the basis for this report. In particular, the authors wish to thank Clarence Sakamoto, Louis Steyaert, Sharon Le Duc, Gary Johnson, Albert van Dijk, Anne Marie Kaylen, and Susan Callis for their contributions. Much of the material on the Normalized Vegetation Index came from Albert van Dijk's Ph.D dissertation. In addition, Russ Ambroziak, while heading CIAD, contributed much of the material on satellite imagery and served as the catalyst for producing this report. He was behind the development of the IHS color interpretation methodology (ACCS). Alan Karnovitz and Ted MacKechnie of CIAD also contributed to the report. The authors wish to thank Jacob Robinson for his patient and exacting work editing the figures. Samita Watson helped prepare the manuscript. The U.S. Agency for International Development (USAID) has provided financial support for the assessments since 1977. Special thanks go to Paul Krumpe, USAID/Office of Foreign Disaster Assistance, who was the focal point of program development. Without his support and encouragement the assessment effort would not have existed.

ASSESSMENT OF CROP CONDITIONS IN AFRICA

EXECUTIVE SUMMARY

Because their livelihood, and sometimes their lives, depend on agriculture, the rural populations in semi-arid regions of Africa are extremely vulnerable to the effects of drought. The severe food shortages which followed the African droughts of 1972-73 and 1983-84 underscored the role that weather and climate play in Third World food supplies. Consequently, international and domestic agencies, both private and governmental, have increasingly emphasized the importance of drought monitoring programs. Early detection of drought can result in actions that offset the effects of failed crops, even to the extent of preventing famine.

This report describes the techniques developed and used at the Climate Impact Assessment Division (CIAD) of the Assessment and Information Services Center (AISC) in support of the U.S. Agency for International Development's drought early warning program. The program was designed to detect drought and resulting crop failure in the countries within Africa's Sahel and Horn regions. Weather and satellite data were used to produce qualitative reports on crop and pasture conditions during the growing season. In addition, near the end of the 1985 and 1986 growing seasons, quantitative yield forecasts were made for rain-fed sorghum and millet crops for administrative regions within each country.

New tools and methods were developed to analyze crop conditions. Meteosat cloud imagery was used to produce rainfall estimates in data-sparse areas. Radiance data from the NOAA-9 satellite were used to produce color imagery representing health and vigor of vegetation. Additionally, a vegetation index derived from the infrared and visible bands of the NOAA-9 satellite was used to indicate growing conditions for one-half by one degree grid cells across the region. Smoothed time-series graphs of the index were used as one tool to assess crop and grassland development during the course of the growing season. Historical yield and monthly rainfall data were used to develop regression equations and forecast cereal yields. The vegetation index was also used to make quantitative yield projections.

Satellite data integrated with ground reports were shown to be effective in drought detection and crop condition assessment for the Sahel/Horn region of Africa and should be evaluated for application to other semi-arid, tropical areas of the world. The vegetation indices and imagery used at CIAD provided information on spatial and temporal changes in vegetative vigor which helped analysts detect likely areas of poor crop growth. Both the rainfall and vegetation index yield models showed promise, with good agreement between their forecasts and reported yields in several countries.

PART I: INTRODUCTION

1. PURPOSE OF THIS DOCUMENT

This document describes CIAD techniques for using weather information to assess crop and pasture conditions in Africa. Included are discussions of data sources, tools for data gathering, data management methodology, and the analytical methodology which is the heart of the process. The result, it is hoped, is a useful overview of ideas and approaches to the use of satellite technology and weather data. This document is especially aimed at meteorologists, statisticians, and agronomists who use weather and satellite data to detect and evaluate anomalous growing conditions in semi-arid regions of the world.

The focus of assessments in CIAD has been agriculture in the developing world, most particularly Africa. Therefore, the tools and methods used are uniquely suited for assessment of weather impacts on agriculture in that region. As its title indicates, this document shares that orientation, although much that is presented also has applicability to assessment methodology in other contexts. The authors hope that these techniques, developed for USAID's Drought Early Warning Program (Sakamoto and Steyaert, 1987), will benefit others monitoring agriculture in Africa or elsewhere in the developing world. While an attempt has been made to present a comprehensive overview of how these techniques were developed, this work is not intended to be an exhaustive summary of the methodologies discussed, but rather a guide to some techniques which have been found to be effective.

2. HOW THIS DOCUMENT IS ORGANIZED

The assessment process at AISC is essentially a distillation of information (Figure 1). Through a series of interrelated steps, various types of raw data are reduced to useful information, from which analysts can draw conclusions about potential consequences. Where necessary, preventive or remedial measures can then be recommended. This process by its nature involves the integration of several disparate but complementary methodologies. The organization of this document reflects that fact. The introduction (Part I) is followed by a presentation (Part II) of the various components of the assessment process as used at AISC. Part II details several independent approaches to the acquisition and use of rainfall and satellite vegetation data to produce assessments of crop and pasture conditions. Part III discusses the integration of these various components into an assessment document or product. Part IV presents conclusions and recommendations for future work.

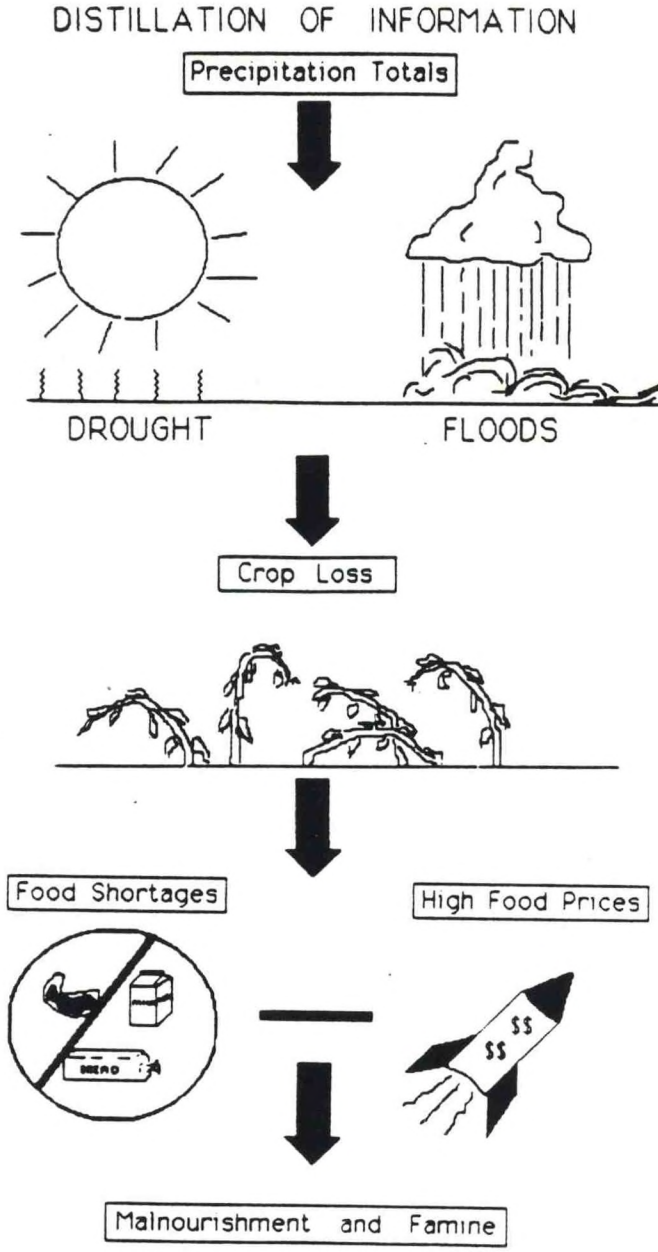

FIGURE 1. The assessment process in Africa is essentially a distillation of information. For example, rainfall totals are used to determine areas affected by dryness and wetness. Potential crop losses could lead to food shortages and higher prices. Areas susceptible to resulting malnourishment and famine could then be identified, so that preventive measures might avert disaster.

PART II: ASSESSMENT METHODOLOGY

1. RAINFALL INFORMATION

In the African countries just south of the Sahara, rainfall is the key factor in explaining interannual variability of food crop production. Less than 15 percent of the crops are irrigated, so crops are extremely dependent on natural rainfall, nearly all of which occurs from May through October. Though temperature is also a critical factor, it is so closely correlated (negatively) with rainfall in this region that rainfall alone can be used to obtain an initial assessment of the impact of weather on crops.

A major activity of crop and rangeland assessment is, therefore, determination of available moisture through monitoring and analysis of rainfall. The following sections discuss methods to acquire, compile, and analyze rainfall information used to assess the condition of agriculture in the Sahel/Horn countries of Africa.

1.1 STATION REPORTS

The three primary sources of station reports are as follows:

1) GTS data. These data are collected by the national meteorological services and transmitted electronically through the World Meteorological Organization's (WMO) Global Telecommunications System (GTS). NOAA's Climate Analysis Center (CAC) quality controls the data, which are usually transmitted every three hours. Additionally, CAC produces "enhanced" 24-hour values based on a technique which uses reported present and past weather codes to estimate missing precipitation values (Thomas and Patterson, 1983). The data are downloaded daily from the NAS/9040 computer in Suitland, Maryland to the AISC VAX 11/780 computer, where they are aggregated to the agroclimatic region level. Data from weather stations within and adjacent to a region are weighted according to reliability and proximity. Monthly "CLIMAT" data are also available through the GTS.

2) AGRHYMET data. These are decadal (10-day) rainfall reports telexed from the AGRHYMET Regional Center (ARC) in Niamey, Niger. They are received one to two weeks after the data are collected in Niamey, but are usually more accurate than the GTS data.

3) USAID Mission data. The Missions provide decadal or monthly rainfall data three or more weeks after the data are collected. These data are also more accurate than the GTS data.

1.2 THE USE OF SATELLITES IN ESTIMATING RAINFALL

Timely assessment of weather impacts requires remote sensing information to estimate rainfall in some countries of Africa. Current (GTS) data are sparse or non-existent from, for instance, Somalia, Sudan, Chad, and Gambia. Observations are taken in these countries but are not reliably transmitted through the GTS. In addition, data transmitted through the GTS are frequently erroneous, so another real-time source of information is needed to supplement the reports.

For this purpose, AISC uses data from the European Space Agency's Geostationary Meteorological Satellite (Meteosat) to estimate rainfall from cloud type and coverage. For sparse or non-reporting areas such as Sudan, this is the principal method of obtaining rainfall information.

The Meteosat-derived rainfall estimates are also compared with the mean outgoing longwave radiation map published weekly by the Climate Analysis Center (Gruber and Krueger, 1984). Low levels of outgoing longwave radiation are generally associated with rainfall occurrences (Motell and Weare, 1987).

1.2.1 The Meteosat Cloud-indexing Technique

AISC has found simple cloud indexing techniques effective for monitoring rainfall in tropical countries. These techniques, which assign weights to cloud types according to the probability of precipitation from each type (Barrett, 1970; Follansbee, 1973), assume that rainfall amounts within an area are proportional to cloud coverage. In climates where the bulk of precipitation is derived from thunderstorms, this technique is surprisingly accurate, as well as simple to use, because cumulonimbus clouds are relatively easy to identify on infrared (IR) satellite imagery.

The quantitative estimation technique used at NOAA/AISC (Callis and Le Comte, 1987) is based on the principle that the area-averaged rainfall amount in a given time period is a function of: 1) cloud brightness (or cloud type), 2) fractional coverage of precipitating cloud, 3) time of the year, and 4) climate regime. In practice, analysts examine infrared images received from facsimile to determine mean daily coverage of precipitating cloud types over agroclimatic regions. Since bright-appearing clouds have the lowest cloud-top temperatures, greatest vertical extent and, presumably, the highest rainfall rates, emphasis is placed on delineating the area encompassed by the brightest clouds on the images. The resulting daily cloud index, obtained from 6-hourly Meteosat images, was used to develop equations which give rainfall amounts as a function of cloud cover. These equations are curves characterized by increasing slope at higher values of mean daily cloud cover.

A sample equation (curve) follows:

$$R_{24} = 15.53\ x + 22.94\ x^2 + 122.57\ x^3 - 69.39\ x^4$$

where R_{24} = 24hr. area mean rainfall (mm)

x = mean daily cloud cover of cumulonimbus (in tenths, from 0 to 1)

This equation is valid for areas in Africa with mean monthly rainfall of 65-150 mm. To adjust for climate differences, the right side of the equation is multiplied by an adjustment factor k equal to $0.45+.00053\ R_a$, where R_a is the mean annual rainfall. This adjustment was designed so that it is equal to 1.0 for mean annual rainfall of 1040 mm. The cloud cover value, x, is the mean fractional coverage of cumulonimbus (bright white clouds on IR imagery) taken from four Meteosat images six hours apart. The resulting rainfall estimate applies to an agroclimatic region, an area with roughly similar climate conditions for crops. The regions vary in size depending on the country (Figure 2). Most countries in Africa are divided into two to six such regions. Cumulus congestus clouds (grey color on IR imagery) are given 40 percent the weight of cumulonimbus clouds. Visible band imagery (where brightness is a function of cloud depth rather than height) is used to help identify cloud type.

The values of the constants of the polynomial equations depend on the long-term mean ("normal") rainfall for the current month; as a result, a family of three curves (Figure 3) was derived empirically to adjust for seasonal rainfall tendencies. Higher "normal" rainfall produces higher daily rainfall estimates. This adjustment arose from observations that, in the Sahel countries, highly reflective clouds early in the year yield less rainfall on the ground than similar-appearing clouds during the peak of the rainy season. This is because low-level dryness causes more evaporation of the rain before it reaches the ground when the rainy season is not yet established. The greater prevalence of cirrus not associated with convection during the dry season also can cause overestimation of rainfall if seasonal or humidity adjustments are not made (Turpeinen et al., 1987). In the absence of detailed data on atmospheric moisture content, the monthly rainfall "normals" provide a simple correction using widely available data. In addition, the climate adjustment factor increases the estimates for areas with annual rainfall above 1040 mm, while estimates are reduced for areas with drier climates.

Verification of satellite estimates against ground reports for eight regions in Sahelian Africa during the 1985 growing season resulted in a correlation coefficient of .83 for 10-day estimates and .95 for the season. Though these results are quite promising, there are some instances where the estimates differ markedly from surface reports. Results for east African coastal countries are poor. Onshore flow in these areas can produce abundant rainfall amounts from relatively warm (grey on infrared)

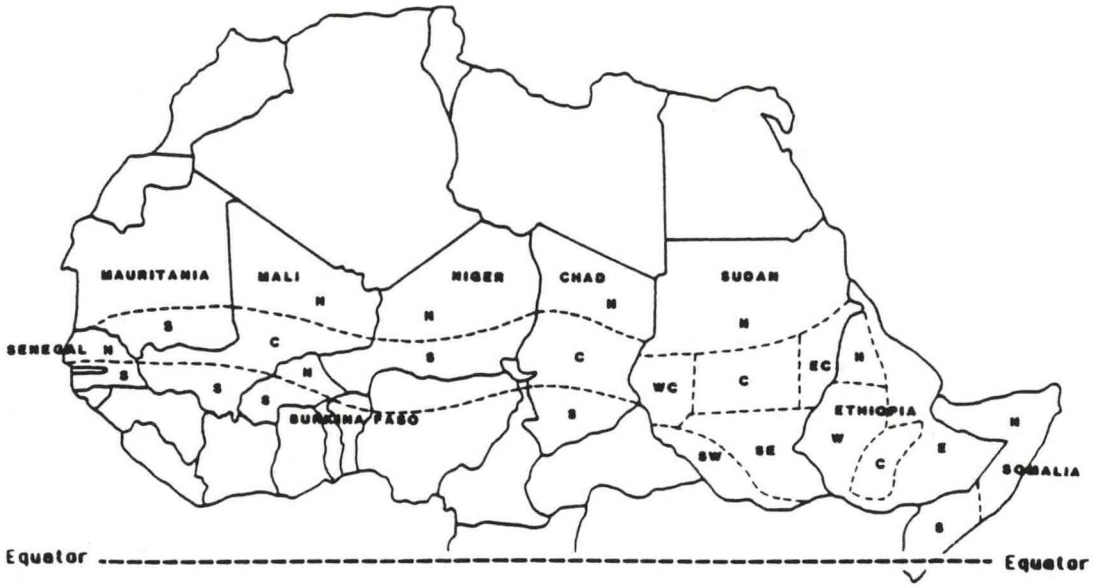

FIGURE 2. The agroclimatic regions for which rainfall estimates are made. The regions are designated North (N), South (S), Central (C), West (W), East (E), etc. as appropriate.

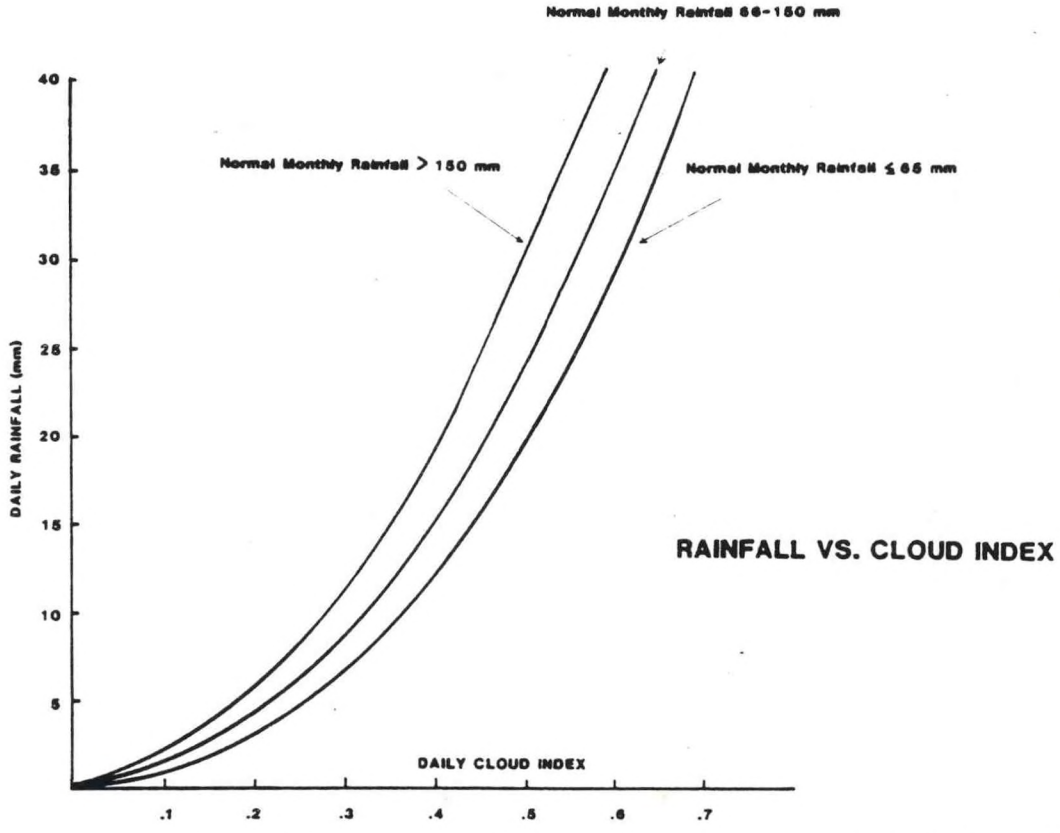

FIGURE 3. Daily regional rainfall (mm) versus cloud index for three ranges of normal monthly rainfall. The curves are derived from plots of rainfall reports versus cloud indices for selected agroclimatic regions in West Africa.

clouds which would usually contribute little rainfall elsewhere in Africa.

In addition to the Sahel countries, Ethiopia and the interior countries of southern Africa (e.g., Zimbabwe, Botswana) appear to be good candidates for successful use of satellite estimation techniques. This type of system works well in other tropical areas, though further climatic adjustments are required outside of Africa.

1.2.2 Satellite Point Rainfall Estimates

As described, AISC has had promising results with an area rainfall estimation technique using four Meteosat images per day, where climate corrections are applied and an expert analyst determines fractional coverage of rain-producing clouds. There are numerous other estimation methods, ranging from much more sophisticated (Griffith et al., 1976) to much simpler (Garcia, 1981). Some of these estimate rainfall amounts for specific locations rather than mean amounts over an area.

As local droughts can cause serious food shortages in Africa, point rainfall estimates are required to delineate the location and extent of areas with rainfall deficiencies. The Meteosat technique for agroclimatic regions is usually adequate for analyzing impacts over broad agricultural or pastoral zones. For detecting local crop problems, experience indicates that analysts need to analyze weather and crop conditions at a resolution closer to 100 km. In mountainous terrain typical of Ethiopia, even higher resolution is required to detect the potential for local food shortages. To meet these requirements, techniques which combine station weather reports with satellite estimates for points or grid cells should be used.

One simple but effective technique incorporates a daily map of reported rainfall totals and three- or six-hourly Meteosat images taken from facsimile machines. An analyst outlines the areas of significant rainfall (as determined from the satellite) on a computer-plotted map of 24-hour rainfall totals transmitted by the WMO GTS. In this manner, satellite-derived information augments the GTS station reports and aids the analyst in defining rainfall boundaries. In areas where stations are widely scattered, this type of satellite information is extremely useful.

Careful plotting of rainfall boundaries, even without knowledge of exact rainfall amounts, can determine the extent and even the severity of drought in small areas. Such plots or "envelopes" indicate locations which have had long periods without rain during critical growing stages for corn or other grains. This simple technique has been of great practical value in southern Africa. Just two weeks of negligible rainfall during corn's tasseling stage in Mozambique, Lesotho, or Zambia can cause irreversible crop damage. Careful monitoring of Meteosat imagery during the growing season has enabled AISC to delineate

areas in these countries that are most vulnerable to crop losses and the consequential food shortages.

With knowledge of rainfall climatology, analysts can use cloud boundary plots to indicate potential rainfall amounts. In Africa's Sahel, rain falls with a mean intensity of 4 mm/h, except at the beginning and end of the season (Cocheme and Franquin, 1967). Estimating the duration of rain at a point using satellite imagery and multiplying by the mean intensity can yield a rough indication of potential rainfall. Alternatively, in an area where the mean rainfall per rainy day is fairly constant (about 14 mm/day in the Sahel), the analyst can simply make a yes-or-no rainfall determination and assign this value to the point in question. All such estimates can be improved by subjective modifications based on cloud appearance.

1.2.3 Using Biomass Imagery

Cumulative seasonal rainfall data derived from cloud imagery or surface reports can be refined with information derived from satellite ground imagery (Ambroziak, 1986).

In dry regions of the world, biomass (the amount of green vegetation) and rainfall are related (Todorov et al., 1983; Tucker et al., 1983). Rain produces biomass of some sort. If the rainfall is continual over a period of months, the amount of added biomass will be nearly proportional to the cumulative rainfall for the period. This relationship is characteristic of the drier regions of the world. For example, in the African Sahel, the soil moisture is near zero at the start of the rainy season. Almost all growing vegetation depends on current-year rainfall. Even in the non-desert regions perennials, which can draw moisture from sub-surface levels, are affected by the current year's rainfall and may become dormant in dry years. Seed is not a limiting factor because even the Sahara desert is covered with windblown seed, and the desert blooms profusely when a rare thunderstorm wets its surface.

In dry areas, the biomass correlates well not only with the seasonal rainfall, but also with crop yields. Satellite imagery modified with the Ambroziak Color-Coordinate System (ACCS) (Ambroziak, 1984) to enhance vegetation provides a visual display of biomass distribution and relative amount (discussed in Part II, section 2). Information embodied in such imagery can be used to interpolate rainfall between stations and to identify stations which have either incorrect reports or which are not representative of the area around them.

The colors of ACCS images provide an analyst with the relative condition of the biomass at each point on the image. The image can be thought of as a representation of a three-dimensional surface with a shape indicating the relative amounts of biomass over the area covered by the image, much as a relief map might illustrate surface elevation. The values at any point cannot be determined unless the surface is "anchored" with

accurate values at several points on the surface. Once the surface is calibrated in this way, the value at any point is given by the shape of the surface. Rainfall data can be used to calibrate the biomass surface. Similar values of cumulative rainfall should have similar Normalized Vegetation Index (NVI) values (section 2) and, therefore, similar hues. Recent research using rainfall data from Sudan confirms the close relationship between NVI values and growing season rainfall (Hielkema et al., 1986). Cumulative rainfall amounts can be overlaid on an ACCS image and the biomass contours can then be used to adjust isohyets (Figure 4).

1.2.4 Automated Techniques

Rainfall estimation techniques can be automated using digital infrared satellite data. Numerous studies (see Arkin and Meisner, 1987, for example) have shown a strong correlation between the amount of area covered by cold cloud tops (effective black body temperature 235°K or less) and rainfall amounts. Milford and Dugdale (1986) have shown promising results using digital hourly Meteosat data, correlating the duration of cold clouds under 223°K with Sudan rainfall.

AISC has not had access to digital Meteosat data. Preliminary tests of automated techniques were made using polar orbiting satellite data on magnetic tape. These tests were not successful. Polar orbiter data are limited to two images daily, so the time of the image is critical. A satellite such as NOAA-9, which produces early afternoon images, misses the usual diurnal rainfall maximum in tropical countries. AISC previously had surprisingly accurate results (with non-automated techniques) for the Sahel countries using the NOAA-6 satellite because it produced images at 1930 hours local time, when the clouds from most of the late afternoon convective peak were still visible. Accuracy fell sharply when imagery from the newer satellites was used, since the equator crossing time was five hours earlier. Geostationary satellites, capable of providing images at least every three hours, are greatly preferred for rainfall monitoring.

1.3 DATA MANAGEMENT

Rainfall data from all sources must ultimately be reduced to a single data set which an analyst can use to make agricultural impact assessments. This means getting reliable and meaningful meteorological information from voluminous amounts of data. Adequate management of the data -- quality control, organization, generation of tables and formatted listings -- is essential. This data management problem is not trivial. The analyst, confronted with rainfall data from numerous sources and time periods, must have a way to separate the significant information from the rest.

1.3.1 Description of the System

Central to the data management methodology of AISC is the

WESTERN SAHEL 1984

Contour Analysis of Cumulative Rainfall

May – July

Using Only Station Data

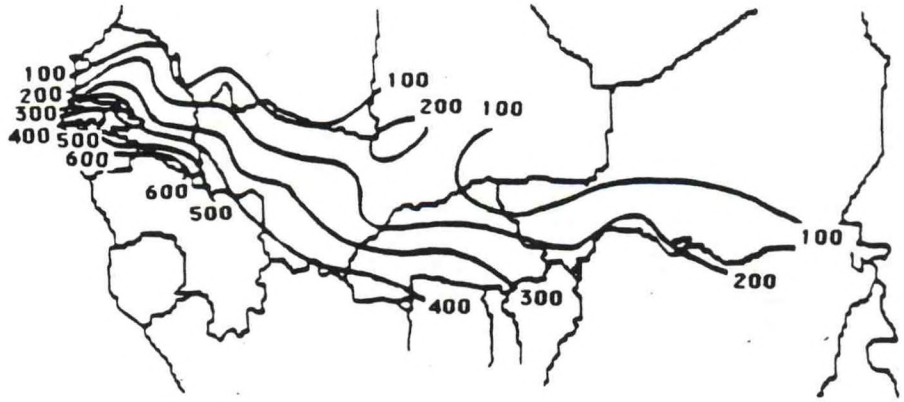

Combining Station Data With ACCS Meteorological Satellite Images

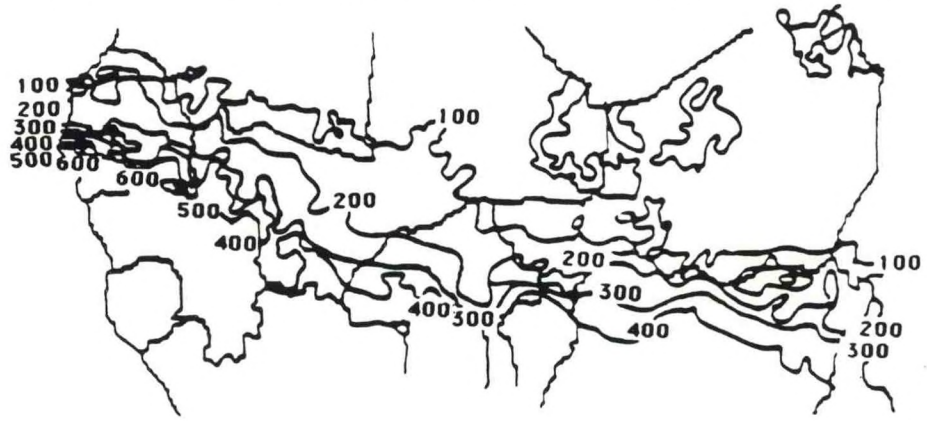

FIGURE 4. Analysis of cumulative rainfall (mm) for May-July 1984 using station data (top map) and station data plus hues from a satellite composite image for July 21-31, 1984 (bottom map).

Comprehensive Area Rainfall Estimation System (CARES). At AISC, rainfall estimates derived by the Climate Assessment Branch (CAB) are used both in the final assessment reports, and by the Models Branch in computer programs which calculate crop indices and rainfall rankings. The Models Branch also maintains the historical data files.

Station rainfall and temperature data are loaded into files on the AISC VAX 11/780 computer and stored for on-line access for one year. Analysts enter cloud cover data for each six-hour period based on visual examination of Meteosat infrared and visible-spectrum images obtained from facsimile machines. The two cloud types entered are cumulonimbus (thunderstorm) and cumulus congestus (showers).

Algorithms compute improved regional rainfall estimates by combining reported rainfall amounts with the satellite estimates. The weighting of the two values -- the average rainfall reported over the region and the satellite estimate -- is determined by a data quality indicator based on the frequency of transmitted synoptic observations. The higher the quality indicator, the more weight placed on the reported rainfall amounts. For areas with few or no observations, the satellite estimate becomes the computed estimate. For areas with relatively complete synoptic reports, the reported rainfall becomes the estimate. Other areas use a mixture of reports and satellite estimates.

Final estimates of rainfall are made for each 10-day period for some 100 agroclimatic regions across Africa. CARES lists the relevant meteorological data on a visual display screen (Table 1). An interactive subroutine allows the analyst to change the computed rainfall estimate if desired. In practice, AISC works with 10-day periods. This time period is short enough to "capture" most significant weather conditions for crops and grasslands in the tropics and long enough to smooth out largely irrelevant day-to-day weather fluctuations.

The display screen provides the analyst with sufficient information to decide whether to accept the computed rainfall value as the final amount. Maps of plotted station data also assist in the decision process.

Figure 5 shows the data used as input for CARES, as well as the products which incorporate the final rainfall estimates.

1.3.2 Final Station Rainfall Estimates

Assessments of weather impacts on crops are based on analyses of station rainfall data; therefore, the purpose of the agroclimatic region rainfall estimates and the cloud envelope analyses is to determine rainfall in areas without reports and improve the quality of the reported or enhanced values received from CAC. For the Sahel/Horn assessments, analysts transmit to the Models Branch final estimates for approximately 130 key stations throughout the region. These stations were chosen

TABLE 1. Sample page for a CARES listing. "ACORN" is code number for the area, country, and region. "FINAL" is the final rainfall estimate (mm) for the August 1-10, 1985 period; the 5th column refers to the normal period rainfall derived at CIAD; column 6 is the percent of normal rainfall; column 7 is the rainfall total derived from weighted, enhanced station reports; column 8 is the satellite rainfall estimate from Meteosat imagery; column 9 is the quality indicator (percent of possible observations received); column 10 indicates the technique used to derive the computed rainfall estimate, with the D and S codes indicating the weights given the enhanced reports (column 7) and the satellite estimates, respectively; column 11 is a rainfall estimate derived from rainfall frequency; columns 12 and 13 give the number of days of rainfall reports and satellite estimates used in the estimates; columns 14 and 15 are the regional observed and normal temperatures (the latter from NWS/CAC data); and the last column is the computed rainfall total.

Period Regional Values: Aug. 01, 1985 - Aug. 10, 1985

-1- ACORN	-2- Country	-3- REG	-4- FINAL	-5- Prcp Norm MB	-6- % Norm	-7- Est.	-8- Sat. Prcp	-9- QUAL	-10- TECH	-11- % Obs Eq.	-12- # Days	-13- # Days Sat.	-14- Tmp.	-15- Temp Norm CAC	-16- Comp
20101	Morocco	N	1	0	100	1		80	DDDD	0	10		25	25	1
20102		S	0	0	100	0		83	DDDD	1	10		26	28	0
20201	Algeria	N	0	0	100	1		68	DDDD	0	10		27	27	1
20202		C	0	0	100	0		68	DDDD	0	10		33	33	0
20203		S	0			0		55	DDDD	0	10		34	31	0
20301	Tunisia	N	0	0	100	0		78	DDDD	0	10		27	26	0
20302		S	0	0	100	0		71	DDDD	0	10		30	29	0
20401	Libya	N	0	0	100	0		76	DDDD	0	10		27	26	0
20402		S	0	0	100	0		65	DDDD	0	10		31	30	0
20501	Egypt		0	0	100	0		61	DDDD	0	10		30	29	0
20601	W. Sahara		0	0	100			0	NNNN						0
20701	Mauritania	N	2	18	10	14		55	DDDD	2	10		30	30	14
20702		S	26	39	66	32	20	53	DSSS	13	10	10	30	29	23
20801	Mali	N	1	10	6	1		53	DDDD	3	9		31	30	1
20802		C	40	67	59	38	41	56	DSSS	24	10	10	29	28	40
20803		S	111	96	117	115	75	49	DSSS	59	10	10	27	26	85
20901	Niger	N	10	21	50	14		74	DDDD	10	10		31	30	14
20902		S	36	67	54	46	37	70	DDSS	37	10	10	29	27	42
21001	Chad	N	0	10	0			0	NNNN						10
21002		C	68	68	100		68	0	SSSS			10			68
21003		S	116	88	132		116	0	SSSS			10			116
21101	Sudan	N	0	11	0			0	NNNN						11
21102		WC	45	65	70		45	0	SSSS			10			45

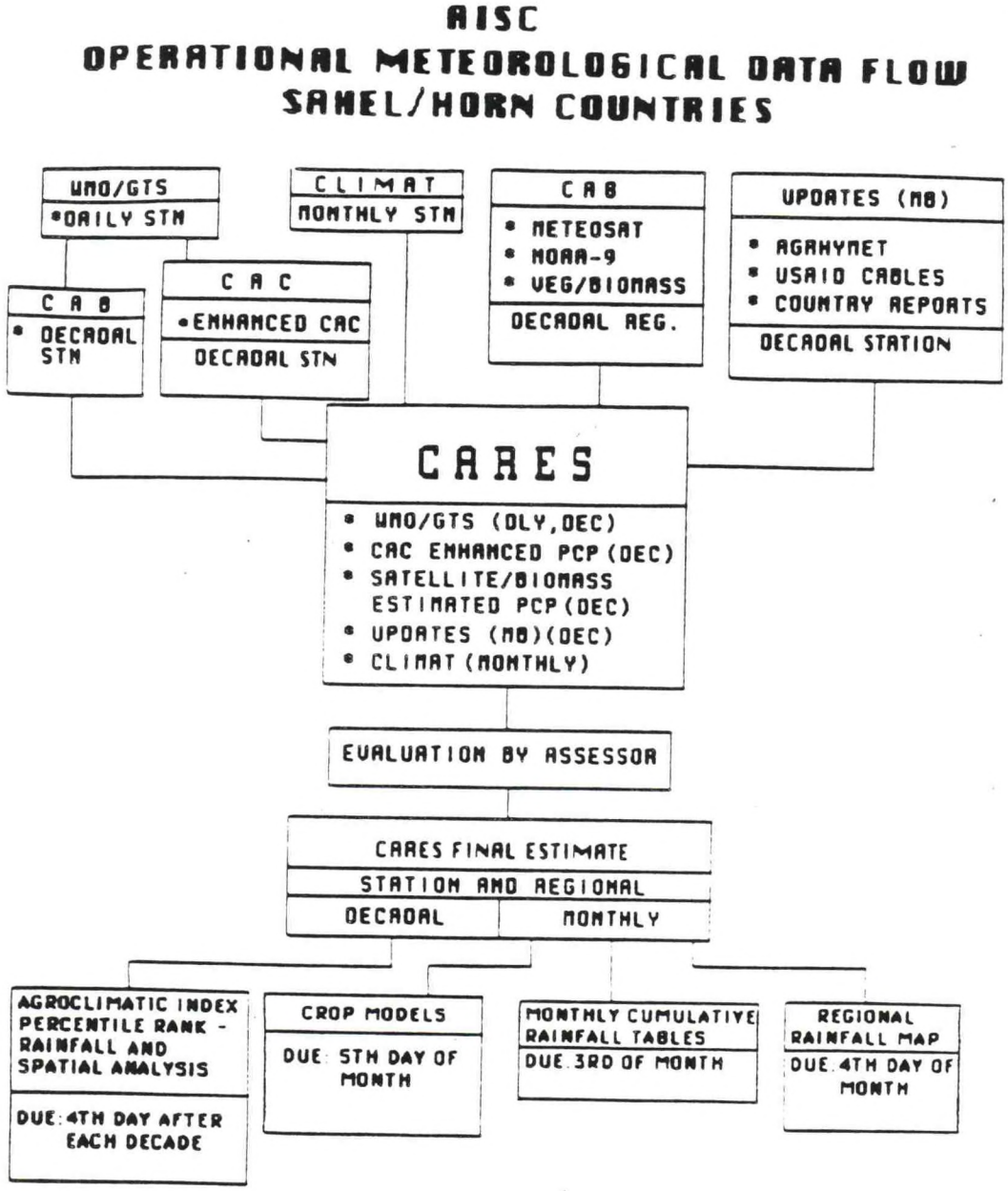

FIGURE 5. The operational flow of rainfall data. The primary source of current daily station (STN) data is the World Meteorological Organization's (WMO) Global Telecommunications System (GTS). The Climate Assessment Branch (CAB) obtains this data from the National Weather Service's Climate Analysis Center (CAC). A source of monthly data is the CLIMAT reports also transmitted over the GTS. The CAB develops rainfall estimates from satellite information, and the Models Branch (MB) collects decadal (DEC) station data transmitted by the AGRHYMET Center in Niamey and other sources in Africa. The Comprehensive Area Rainfall Estimation System (CARES) helps to organize and integrate the data so as to produce station and regional rainfall totals used in crop models and other products shown at the bottom of the diagram.

according to the availability of current and historical rainfall data and their location in or near important crop areas.

Where the CAC-enhanced 10-day totals are consistent with surrounding reports and satellite images, these become the estimates used for current applications. In the many cases where the reports are missing or suspect, the analyst uses Meteosat data and nearby stations to arrive at a rainfall total. Satellite estimates are based on careful analysis of cloud areas and their position relative to the stations. The analyst prepares daily maps of Africa with a hand-drawn depiction of the location of significant rain areas based on interpretation of infrared and visible imagery, using the cloud envelope techniques previously discussed to derive initial station estimates. These daily estimates are summed for 10-day periods and placed on a map which also displays 10-day totals received from CAC. Additional adjustments to the station satellite estimates follow computation of the regional satellite estimates. A hand-drawn contour analysis can be constructed from the 10-day data. The resulting map helps identify stations with estimates or reports which are suspect. The 10-day values can then be adjusted to conform more closely to the analyzed rainfall pattern. These adjusted rainfall totals are entered into a computer, where cumulative totals for the season to date are calculated and plotted on a large Mercator map of the Sahel/Horn region. The ACCS vegetation imagery for the most recent period is displayed on top of the map using a slide projector. The analyst then uses the station data and the ACCS contours to draw isohyets of cumulative rainfall on the map. The resulting analysis is used to determine areas where "effective" rainfall has been deficient and crop or grazing problems may exist.

The 10-day final station estimates are used by the Models Branch to produce crop indices, percentile rankings, and statistical yield estimates. When the "official" 10-day reports are later received from the AGRHYMET Center in Niamey, Niger, or from the USAID missions in other African countries, they are compared with the estimates. Usually these reported totals replace the estimates and become the final values. Occasionally, the reported total is not accepted because the estimates indicate that the report is either in error or not representative of the area around the station.

As with the regional estimates, the station amounts are available in tabular and map form and are displayed for 10-day, monthly, and season-to-date time periods.

1.3.3 Evaluating Rainfall Reports

Often, there are substantial discrepancies among the GTS reports, the CAC enhanced reports, the AGRHYMET reports, and the satellite estimates. Much time can be spent deciding which value is "correct."

When dealing with rainfall observations in a climate characterized by convective-type rainfall (as opposed to stratiform), it is imperative to keep in mind that a measurement is derived from rain falling over an area of about 325 sq cm, the funnel area of the standard (8-inch) rain gauge. Because of the spotty nature of tropical showers, extrapolating amounts beyond the measurement site is risky. Observers in tropical climates frequently remain dry while witnessing a shower that is occurring several hundred meters distant. Radar studies have shown "the spatial variability of rainfall is so pronounced that a single gauge often does not sample representatively over an area, even one as small as 4 km^2" (Austin, 1987).

What constitutes a "correct" rainfall value depends on the application. For flash-flood forecasting of small streams, a value representing 1-km areas and obtainable only from radar may be required. For monitoring national crop production in Mali, a rainfall value which represents an area more than 100 km wide may suffice. This value may or may not be similar to the rainfall measured at the official observation sites. In parts of Sudan and Ethiopia, tracking rainfall in areas less than 100 km wide is required to effectively forecast the potential for local food shortages.

Ultimately, accuracy of the rainfall estimates can only be revealed by studying the impact of the rainfall on the environment. If there is resulting flooding commensurate with the high estimated rainfall totals, then that fact supplies a measure of "ground truth." If reports of crop growth or losses are consistent with rainfall estimates for Mali and Ethiopia, then they tend to verify the rainfall estimates.

In conclusion, the analyst should be skeptical of rainfall reports from areas with tropical weather regimes. Such reports should be supplemented, if possible, with other information. Satellite cloud imagery and satellite vegetation imagery and indices are valuable tools for determining representative rainfall totals.

1.4 USING WEATHER DATA IN THE ASSESSMENT

Determining the temporal and spatial variation of rainfall during the growing season is a principal step in making qualitative or quantitative agricultural assessments in Africa. Analysis of rainfall includes determination of absolute values as well as values relative to some historical baseline. Absolute values alone give the analyst some guidance on crop conditions, while comparison with a baseline (usually the preceding year or a 10-, 20-, or 30-year mean) reveals the extent to which the current year deviates from a known standard.

The basic graphic tools for making assessments are maps showing accumulated rainfall for the growing season, percent of "normal" rainfall, and percentile rankings. Because of recent climate fluctuations (see, for example, Todorov, 1985) the term

"normal" must always be defined when used in the Sahel countries of Africa (including Sudan). Climatologists tend to use the most recent 30-year period ending with the start of the current decade (currently 1951-80). However, there is evidence that agricultural practices in the Sahel countries have adapted to some extent to the drier climate which began in the late 1960s. An example would be the recent higher cereal yields despite modest rainfall amounts. If this is so, a shorter baseline period -- perhaps 1961-80 -- might be more representative of a meaningful "normal" for the late 1980s.

The type of rainfall analysis useful in the assessment process depends upon the stage of the rainy season. For example, during the early and middle stages, information about departure from "normal" rainfall is important in determining whether the early germination and growth of cereals is "on schedule." For the latter part of the season, cumulative rainfall might receive more emphasis because of its usefulness in making preliminary judgments of general crop and pasture conditions and even yields. In all cases, it is important to know the climatology and the crop calendar of the region under study.

1.4.1 Cumulative Rainfall

For rain-fed cereals in the countries in the African Sahel zone, both informal analyses (Figure 6) and formal studies (see section 4) have shown a high correlation between seasonal rainfall totals and yield. Little or no yield is likely from sorghum or millet with cumulative rainfall less than 200 mm, while the yield tends to increase almost linearly with rainfall from 200 to 700 mm. As a general rule, cumulative May-September rainfall (in mm) approximates millet yield in kg/ha in this range. Thus, a May-September rainfall total of 500 mm gives an approximate yield estimate of 500 kg/ha (0.5 mt/ha). Sorghum estimates tend to be 10 to 20 percent higher. Of course, this is not true for every country in the Sahel and does not take temperature, temporal distribution of rainfall, or technology trends into consideration. Also, maize yields are not as simple to determine, as temporal distribution of rainfall during the season, and especially during tasselling, is more important with this crop.

Cumulative seasonal rainfall is such an important indicator of agriculture in the Sahel countries that a map of total rainfall for the season can easily be converted to one showing crop and grassland conditions. The AGRHYMET Center in Niamey, Niger, publishes a map showing cumulative rainfall for April-October on which isohyets serve as boundaries for quantitative and qualitative yield estimates (Figure 7). On this map, five rainfall ranges are used to indicate yield estimates for pastures, cowpeas, millet-sorghum, groundnuts, and maize. Rainfall totals of 200-300 mm, for example, translate to fair-to-average yields for pastures and cowpeas and poor-to-fair yields for millet-sorghum and groundnuts. No yield for maize is expected with such low rainfall. Millet-sorghum yields are given

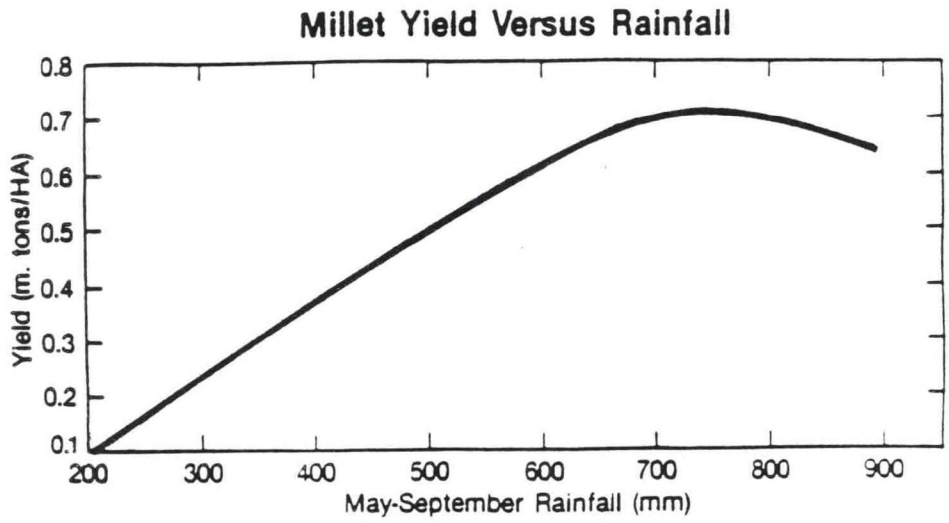

FIGURE 6. A schematic of the relationship between seasonal rainfall and millet yield in the Sahel countries.

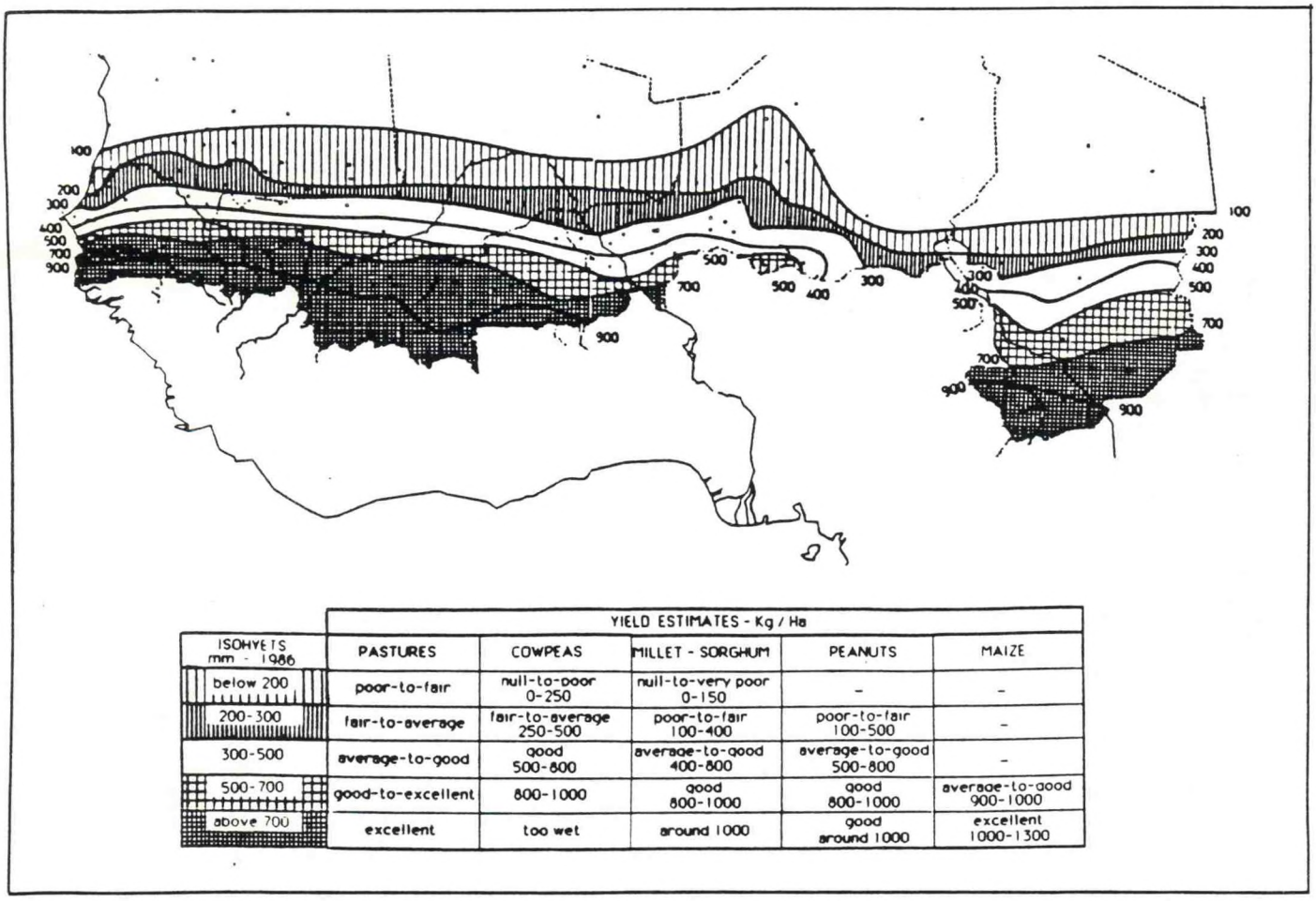

ISOHYETS mm - 1986	YIELD ESTIMATES - Kg / Ha				
	PASTURES	COWPEAS	MILLET - SORGHUM	PEANUTS	MAIZE
below 200	poor-to-fair	null-to-poor 0-250	null-to-very poor 0-150	-	-
200-300	fair-to-average	fair-to-average 250-500	poor-to-fair 100-400	poor-to-fair 100-500	-
300-500	average-to-good	good 500-800	average-to-good 400-800	average-to-good 500-800	-
500-700	good-to-excellent	800-1000	good 800-1000	good 800-1000	average-to-good 900-1000
above 700	excellent	too wet	around 1000	good around 1000	excellent 1000-1300

FIGURE 7. Crop and pasture condition assessment based on cumulative rainfall, April-October, 1986. Source: Bulletin Agrometeorologique Decadaire Regional Pour les Pays du CILSS, October, 1986.

as 100-400 kg/ha.*

1.4.2 Normals and Departures from Normal

Rainfall totals alone give the analyst an approximation of crop and pasture conditions, while departures from baseline values such as normals add historical perspective. The departures also can indicate potential food shortage problems. Food production and supplies tend to be attuned to "normal" weather conditions. Large departures from expected weather conditions, especially warm and dry anomalies, can result in yield reductions that eventually require emergency food shipments. Except in those few countries where rainfall normally exceeds optimal growing requirements, reports of unusually low agricultural yields begin appearing when growing season rainfall is less than 80 percent of "normal." The hydrological practice of defining as drought years those years which accumulate 75 percent or less normal rainfall applies well to most of Africa; impacts to agriculture at this level of rainfall deficit often lead to considerable apprehension among farmers and planners. At or below 60 percent of "normal" rainfall over the course of the growing season, major crop losses usually result, and the risk of food shortages is great in susceptible areas.

1.4.3 Historical Rankings

Percentile rankings are valuable analysis tools for semi-arid areas in Africa. Climatic fluctuations and high year-to-year variability make rainfall statistics such as mean and median highly dependent on the choice of time period. AISC uses historical 10-day station data to calculate percentile rankings throughout the growing season. Maps are prepared depicting the rankings, rainfall totals, and the percent of normal based on 1961-80 data (Figure 8). This information gives the analyst an excellent historical perspective of the current season's rainfall. In general, the severity of the impact is commensurate with the severity of the anomaly.

It is especially informative to relate the current year's anomalies to an analogue year. Comparison of the current season to one characterized by memorable food shortages, for example, is an extremely effective means of communicating potential impacts to the users of the assessment. In the Sahel countries, the drought years of 1973 and 1984 are remembered as years which featured widespread crop losses and food shortages. If the current year is similarly dry, an assessment which draws the appropriate analogy can impart more useful information than one which simply quotes statistics on rainfall totals and water balance indices.

---

* The reader will note that yields are not consistent with those in the graph in Figure 6. This is due in part to the inclusion by AGRHYMET of sorghum crops and some data from higher-yielding areas.

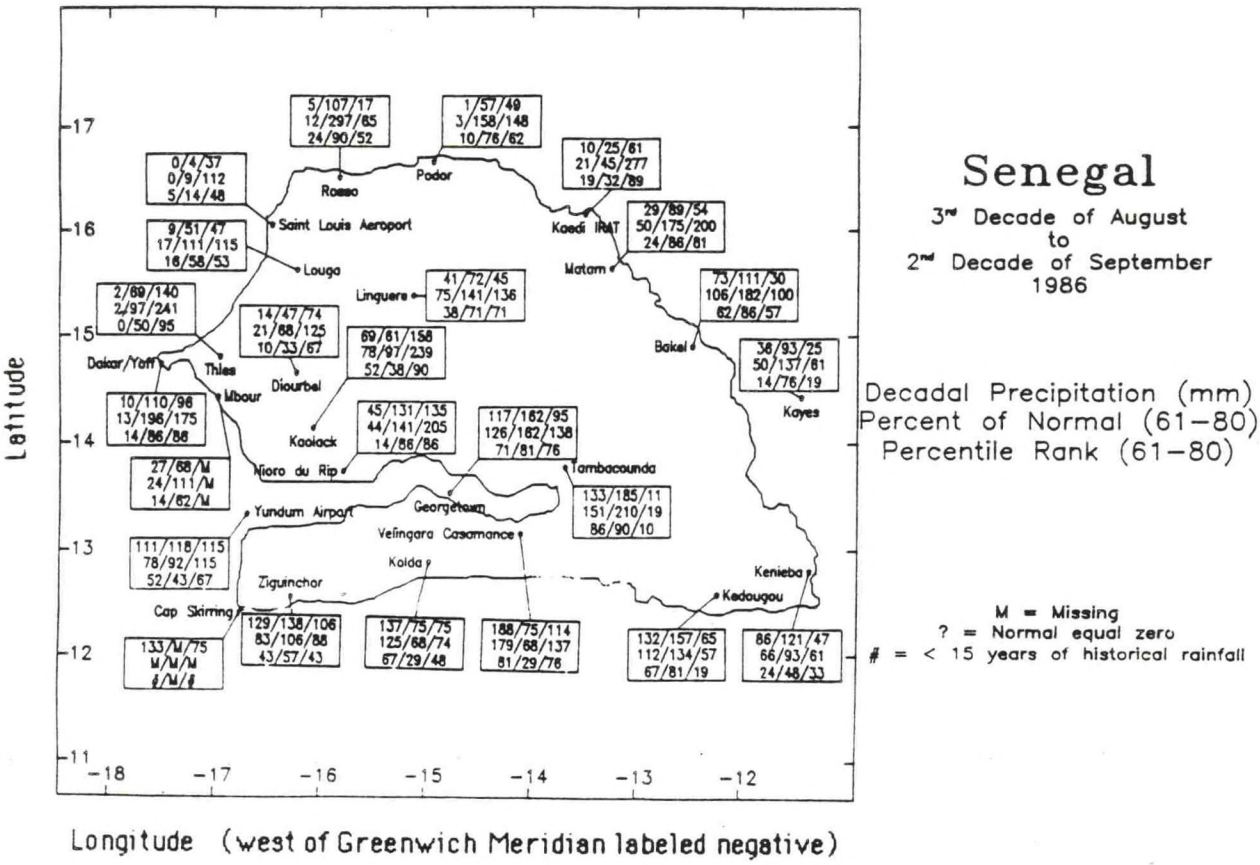

FIGURE 8. Map showing station rainfall for August 21-31, September 1-10, and September 11-20, 1986, in Senegal. The second row of numbers depicts rainfall as a percent of normal; the bottom row depicts the percentile rank.

2. REMOTE SENSING FOR VEGETATION MONITORING

2.1 INTRODUCTION

NOAA Advanced Very High Resolution Radiometer (AVHRR) data are one of the main sources of information used for assessment of crop conditions. Satellite data are used in two principal forms: 1) satellite images and 2) Normalized Vegetation Index (NVI) products (i.e., comparative maps, time-series plots, etc.). Whatever the form of representation of satellite data, the user must have an understanding and appreciation of the nature of the data processed and principles of remote sensing as applied to monitoring crop condition.

A complete remote sensing system must perform a full sequence of operations ranging from data collection, to preliminary processing, through data analysis and interpretation to, finally, presentation of thematic results.

Data collection begins with sensors. "Sensor" covers a wide range of devices (e.g., cameras, scanners, radars) used to collect and record information about objects. Sensors are carried by platforms such as aircraft, balloons or satellites. They detect electromagnetic radiation (EMR) which is recorded as a digital signal and later transformed into analog data.

Polar orbiting satellites do not actually photograph the earth's surface. Rather, for each discrete element of the earth's surface scanned by the satellite, the satellite's Advanced Very High Resolution Radiometry system obtains five numbers. Effective interpretation of these data is possible only if the data are timely and processed into a form suitable for use by analysts. For example, the data might be ordered and compiled into tables and charts for use by analysts. Or various mathematical "indices" might be defined and studied. Or a visual image might be constructed by representing each scanned area of the earth's surface with a colored point on a picture or computer video display. The color could be assigned according to the data values obtained by the sensors, so that an analyst would have a map-like visual representation of the data. All of these methods are used in CIAD.

The major aspects of the remote-sensing process as it relates to vegetation monitoring are covered in the sections that follow. The section titled "Principles of Remote Sensing Systems" discusses some of the physical principles underlying the use of remote sensing systems. "Methodology" is an overview of methods of adjusting data to make it more reliable for use in vegetation monitoring, and methods of designing and producing visual images for use by analysts interpreting the data. "Real-time Data Acquisition" is a brief outline of the processing of satellite data for the previously-described purposes. The final section, "Principles of Data Interpretation," covers considerations of image and data interpretation, and their interrelationships.

2.2 PRINCIPLES OF REMOTE SENSING SYSTEMS

2.2.1 Radiance

All matter at temperatures above absolute zero (-273°C or 0°K) radiates electromagnetic energy. The hotter the object, the more radiation it emits (Stefan-Boltzman Law). The peak radiation (at a given wavelength) is an inverse function of the absolute temperature of the object. In the case of the sun, the maximum peak of radiation lies at 0.47μm wavelength (according to Wien's Law).

The energy that reaches the earth's surface is absorbed, transmitted, or reflected. These processes keep the earth's surface at an average temperature of about 300°K. The earth itself is an emitter of EMR, but with a much lower energy output and a distribution curve of radiation with a peak near 10μm. This curve stretches from 3.5μm into the microwave region.

In theory, it should be possible to use all of the electromagnetic spectrum between the ultraviolet and very low frequency (VLF) radio waves for remote sensing purposes. However, the earth's atmosphere, composed of water vapor, carbon dioxide, carbon monoxide, nitrous oxide, ozone, and other gases, has a disturbing influence on the propagation of radiation. The result is that only a limited number of "atmospheric windows" of the electromagnetic spectrum are relatively unaffected by atmospheric reflection, absorption, and scattering. Because of this, the present state of the art permits measurements in only a few narrow bands. These include:

- the visible (0.4-0.75μm) and reflective near-infrared (0.75-1.1μm). Data collected in these "windows" are energy reflected by terrestrial objects. Sensors include conventional and aerial photographic cameras and, since the 1960s, multispectral scanners;

- two spectral bands in the medium (thermal) infrared (3-5μm and 6-14μm). The data collected in these "windows" are energy radiated by terrestrial objects. Photo emulsions cannot be used at these wavelengths. Sensors used are scanning devices equipped with detectors sensitive to thermal infrared radiation;

- the microwave region (1 mm to several meters). Sensors used are of two types, active and passive. Active microwave sensors direct a beam to the object of interest and detect the reflected portion of the radiation (radar, for example). Passive microwave sensors detect the very low intensity of radiation emitted at these wavelengths.

To monitor the earth's surface and vegetation for agricultural applications, the most important window is the wavelength 0.4-1.1μm, the visible to near-infrared.

2.2.2 Reflection of the Earth's Surface

Objects on the earth's surface have unique reflectance curves showing the percent of reflectance at different wavelengths. For example, Figure 9 shows the reflectance curve for a healthy green leaf. Reflectance is low, often 10-20 percent, in the visible portion of the spectrum due to high absorption corresponding to the chlorophyll absorption bands. Absorption of blue (0.40-0.47μm) and red (0.60-0.70μm) light is higher than that of green light (0.50-0.54μm). Therefore, reflected light of leaves is seen by the human eye as green. The internal structure of the plant leaf is responsible for the high reflectance in the near-infrared (0.75-1.1μm) spectral region. The reflectance in the 1.3-2.5μm spectral region is mainly controlled by the amount of water in the leaves of the vegetation. Therefore, turgid leaves reflect the near-infrared much more than moisture-deficient or stressed leaves. Various types of foliage have their own reflectance curves controlled by the biological and structural properties of the plant leaves (Figure 10).

Figure 11 shows the reflectance curves as recorded for various soils with different soil moisture content. The spectral reflectance of soils is influenced by: moisture content; amount of organic matter; mineral characteristics; relative percentage of clay, silt, and sand; and soil surface roughness.

In Figure 12 the reflectance curves for a bare soil and stressed and well-watered wheat are shown. In the visible part of the spectrum the soil has a higher reflectance than the wheat; in the near-infrared the vegetation has a higher reflectance than the soil. The spectral signature of wheat is distinctive.

Vegetation development progressively reduces the reflected energy in the visible part of the spectrum and increases the reflected energy in the near-infrared. This process continues until a relatively constant reflectance value for the visible and near-infrared is reached. An index used to characterize vegetation development is Leaf Area Index (LAI), defined as the leaf area per unit ground area. The visible reflectance will decrease and the near-infrared reflectance will increase with increased values of LAI.

2.2.3 Remote Sensing Satellites

For the purpose of this manual, satellite sensors to detect electromagnetic radiation can be divided into two groups: earth resource satellites and environmental satellites.

Earth resource satellites provide low frequency coverage of portions of the earth's surface at a relatively high spatial resolution of about 20-80 m. Examples are Landsat and SPOT.

Environmental satellites provide high frequency global

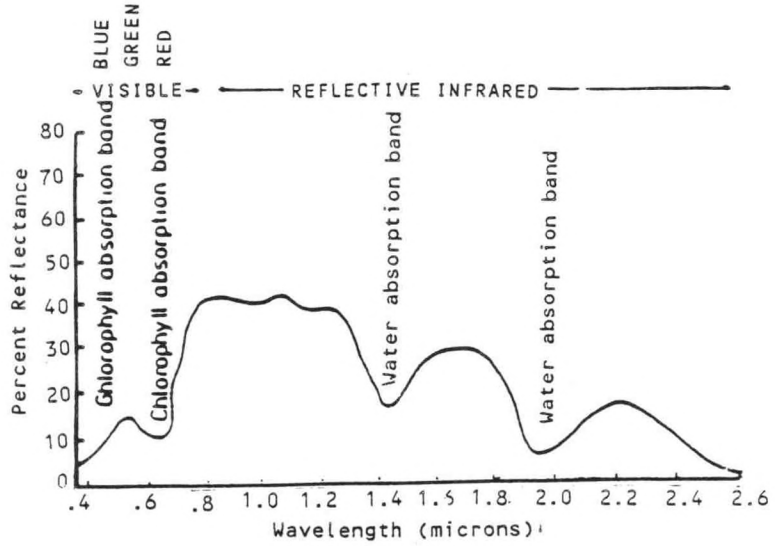

FIGURE 9. Reflection curve for a healthy green leaf. Source: American Society of Photogrammetry, 1975.

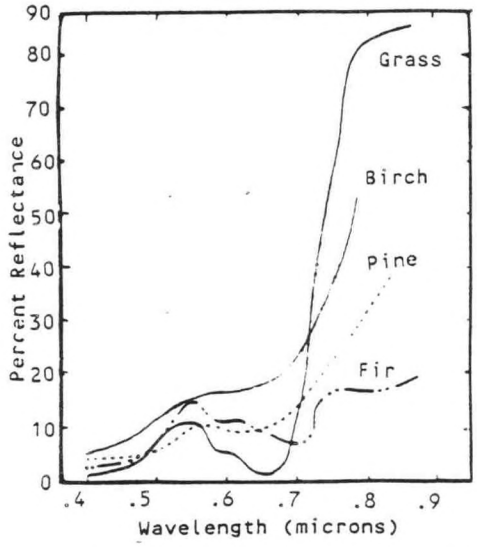

FIGURE 10. Reflection curves for various types of foliage. Source: American Society of Photogrammetry, 1975.

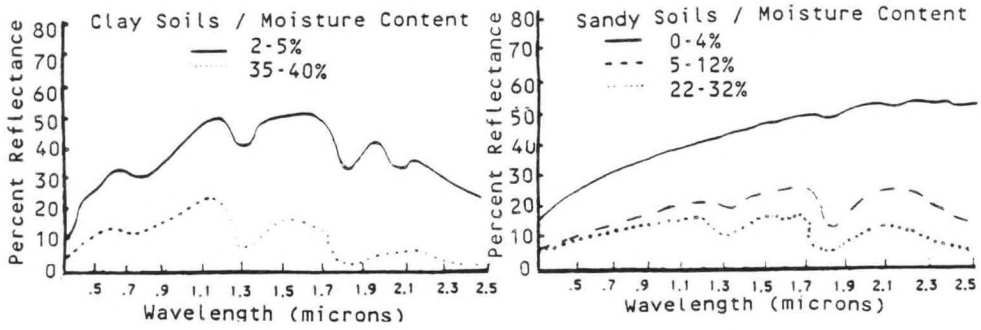

FIGURE 11. Reflection curves for two soil types under different moisture contents. Source: American Society of Photogrammetry, 1975.

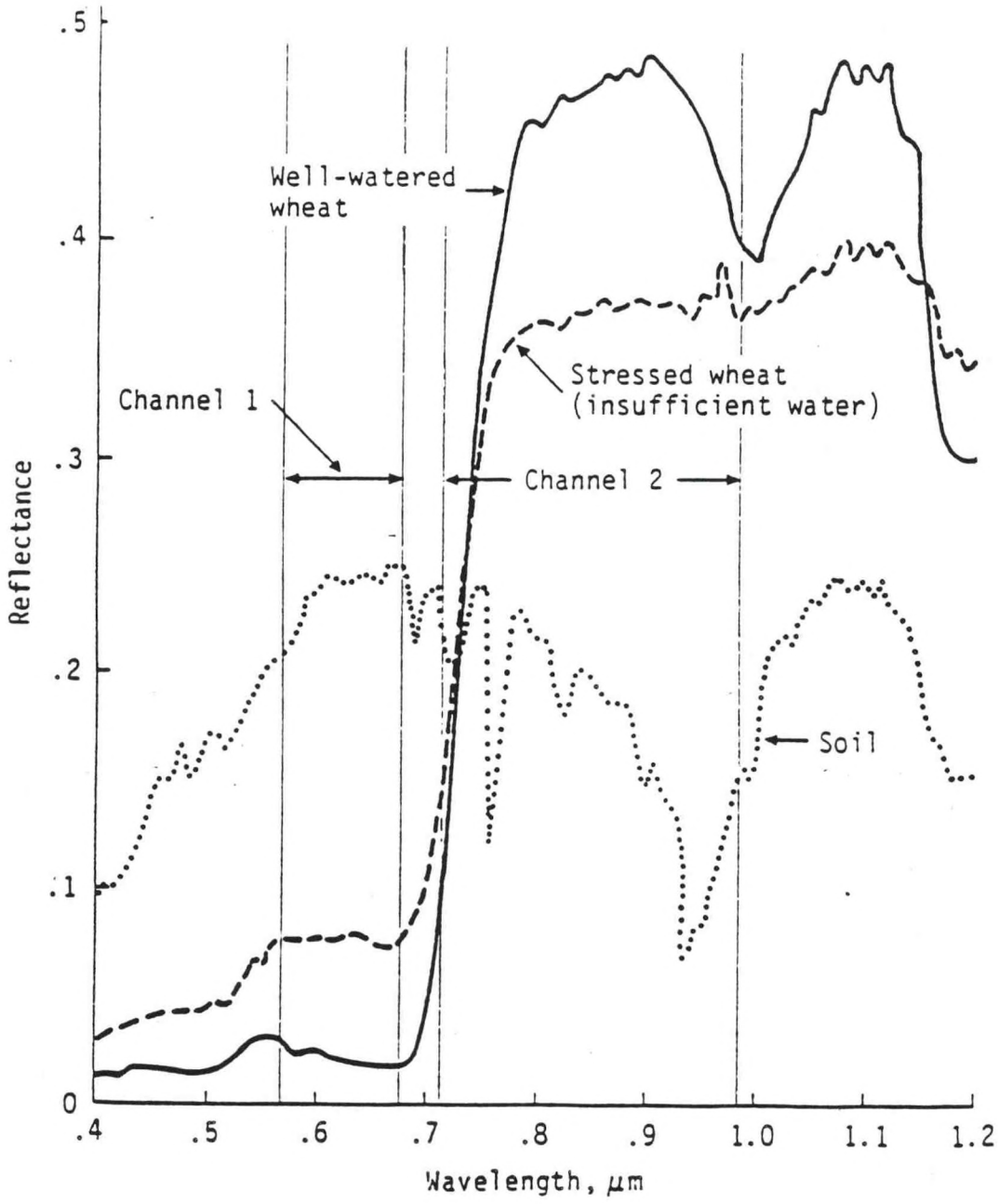

FIGURE 12. Response of wheat across NOAA AVHRR reflective channels. Source: Gray and McCrary, 1981.

coverage at a relatively low spatial resolution of about 1-2.5 km. There are two types of environmental satellites: geostationary and polar orbiting. The geostationary satellites are "locked" in an orbit 36,000 km above the earth's surface. They make one complete orbit above the equator in exactly 24 hours, thus giving the impression of being stationary over a certain point on the equator. Hence, the images produced by a geostationary weather satellite always represent the same part of the earth's surface. Changing meteorological conditions can be monitored effectively by as many as 48 images each day.

The polar-orbiting satellites such as NOAA-9 orbit at a relatively constant altitude ranging between 800 and 1400 km on trajectories passing near the north and south poles (Kidwell, 1986). They pass over the same general area at the same local time every twelve or twenty-four hours. The data of polar orbiting satellites have a higher spatial resolution than the data of most geostationary satellites, so they are more effective for vegetation monitoring.

2.2.4 NOAA Spacecraft Instrument Systems

The four primary spacecraft instrument systems are:

1) Advanced Very High Resolution Radiometer (AVHRR),

2) TIROS Operational Vertical Sounder (TOVS),

3) Data Collection System (DCS), and

4) Space Environmental Monitor (SEM).

Because of its application to monitoring vegetation, only data from the AVHRR instrument will be discussed in this manual. The AVHRR is sensitive in five spectral bands:

Channel 1 (0.55-0.68μm)

Channel 2 (0.725-1.10μm)

Channel 3 (3.55-3.93μm)

Channel 4 (10.5-11.3μm)

Channel 5 (11.5-12.5μm)

Data from the AVHRR are available from the polar orbiting satellite in five operational modes -- four are processed on the satellite, while the fifth is processed on the ground:

1) APT (Automatic Picture Transmission): direct readout to worldwide ground stations of the APT visible and infrared data (4-km resolution).

2) HRPT (High Resolution Picture Transmission): direct readout to worldwide ground stations of the HRPT data for all spectral channels (1.1-km resolution).

3) GAC (Global Area Coverage): global on-board recording of 4-km resolution data from all spectral channels for processing in the NOAA central computer facility at Suitland, Maryland.

4) LAC (Local Area Coverage): on-board recording of data from selected portions of each orbit at 1.1-km resolution of all spectral channels for central processing.

5) Global Vegetation Index (GVI): produced by NOAA/NESDIS since April 1982 from Global Area Coverage (GAC), 4-km resolution AVHRR data, and displayed on a one-sixteenth sub-mesh grid of the standard 65x65 polar stereographic projection grid (Tarpley et al., 1984). Since 1983 an enhanced GVI product has been used.

Application of AVHRR data to the monitoring of crop conditions is based on the GAC and GVI operational modes. The Normalized Vegetation Index (NVI)* is calculated as follows:

$$NVI = (CH_2 - CH_1) / (CH_2 + CH_1)$$

where CH_1 is the visible channel and CH_2 is the near-infrared channel.

2.3 METHODOLOGY

2.3.1 Methods for Filtering AVHRR Data

Successful use of NOAA AVHRR data for vegetation monitoring requires the application of filtering algorithms to minimize the noise and strengthen the target signal. Several filtering procedures fulfill this goal. Most of the procedures reduce the atmosphere interference which attenuates the vegetation signal. These procedures can be summarized as a) indexing the data, b) removing "contaminated" pixels,** c) spatial sampling and averaging, and d) temporal filtering.

Indexing the AVHRR data serves to compress the spectral data, eliminate noise, and extract the maximum information from these data. The Normalized Vegetation Index (NVI) has been

---

* The NVI is often referred to as the NDVI (Normalized Difference Vegetation Index.).

** The term "pixel" denotes a picture element, essentially one visible dot in the satellite image on a computer's color display screen.

demonstrated useful for vegetation monitoring (Schneider et al., 1981; Tarpley et al., 1984; van Dijk et al., 1987).

A thermal cloud mask technique increases the vegetation signal by removing pixels contaminated by clouds. The identification of such pixels is based on the concept that cloud and atmospheric haze have lower temperatures than ground level vegetation. The thermal channel is used to identify such pixels (Tucker et al., 1982). Another indirect way of removing cloud contaminated pixels is using the maximum value composite technique (Holben, 1986). The procedure involves selection of the maximum NVI for each pixel over a chosen time interval (normally 7-10 days).

Spatial sampling and averaging of the data also reduce noise. Although spatial sampling reduces resolution it helps to increase the vegetation signal. In sampling, LAC data are aggregated to GAC-level data which are then aggregated to GVI-level data (Tarpley et al., 1984). Spatial averaging of the data substantially increases the signal-to-noise ratio.

All these techniques are used to minimize noise in the surface reflection signal, but the data are still contaminated. Although trends over a growing season are usually apparent in NVI time-series, there is still a great deal of data fluctuation over shorter periods. Reduction of these fluctuations can be achieved by applying temporal filtering techniques to smooth the data. One such technique is a median filter which not only smooths the data but further reduces the noise (van Dijk, 1986). The resulting product is an additional refinement of the NVI and has proved to be effective for vegetation monitoring.

2.3.2 Methods for Creating Images

Color images derived from vegetation indices can be used to depict vegetation conditions. These images provide an excellent tool for analysts who wish to view both spatial and temporal changes in vegetation growth across the semi-arid regions of Africa.

AVHRR imagery used for agroclimatic assessment is enhanced using a scheme developed by Ambroziak (1986) which remaps the data into intensity, hue and saturation (IHS) color space. Intensity is the perceived brightness or darkness of an object. For example, what we call brown is in fact a lower-intensity orange. Hue is the attribute most intuitively perceived as color, such as blue, green, yellow, or red. Saturation refers to the degree of dilution of a color with white. For example, as red becomes less saturated, it becomes the "color" we call pink; and if completely unsaturated, it becomes white.

The distinguishing feature of the Ambroziak Color-Coordinate System is that the three fundamental color attributes of each pixel -- intensity, hue, and saturation -- are used independently to convey different kinds of information about the conditions

portrayed in the satellite image. In terms of its information content, then, an ACCS image in effect shows more about the underlying data than would a conventional image. The saturation attribute is used to distinguish cloud cover, while intensity is used to make distinctions among pixels with the same NVI, and each class interval of NVI is assigned a different hue so that earth features are "natural" looking. For example, bare soil is red, whereas sparse vegetation is yellow.

Color-coordinate systems fall into two broad groups: those based on the physical principles of color creation (e.g., the additive mixture of green and red results in yellow) and those based on the principles of color perception. The RGB system is based on the physical principle of additive color creation and gets its name from the three additive primaries: red, green, and blue. The ACCS uses the RGB system to represent a wider range of vegetation conditions than might otherwise be possible by remapping AVHRR multispectral data into an IHS color perception system (Ambroziak, 1986) based on independent use of the three attributes -- intensity, hue and saturation -- so that each represents different information about the data. The three most useful AVHRR-derived parameters for monitoring vegetation and detecting atmospheric contamination are: the normalized vegetation index, the maximum reflectances of the visible and near-infrared channels, and a derived temperature from the thermal infrared channel. When these parameters are remapped into IHS color space, the vegetation index is mapped into the hue coordinate, the maximum values of channels 1 and 2 are mapped into the intensity coordinate, and temperature is mapped into saturation.

The remapping procedure entails two steps. The first is the plotting of individual reflectance values of the visible and infrared channels (Figure 13) on an X-Y cartesian grid. On the graph, lines of equal NVI radiate from the origin and each class interval of NVI is assigned a different hue so that earth features are "natural" looking. Bare soil is red, stressed or sparse vegetation is yellow, lush vegetation is green or blue, and so on. Negative NVI values are plotted in a single hue.

In the second step, saturation at a point (x,y) is adjusted by adding white to the hue, based on the y-coordinate value, denoting temperature (Figure 14). Saturation is used as a cloud filter. When Channel 4 or 5 thermal data are not available, visible reflectance values are used to set saturation. Pixels with higher visible reflectance are assigned lower saturation. As a result, bright visible pixels (clouds, sand) have a lot of white, while dark visible pixels (water, lush vegetation) have deep, rich hues. In other AVHRR scenes, the 10.5-11.3μm thermal band (Channel 4) is used in a similar manner. Lower temperatures have a lower saturation while higher temperatures have a higher saturation. Cold clouds are white; higher elevations and warm clouds have a pale color; and the warm lowlands have a deep, rich color. Thin cirrus clouds (which are very cold but do not

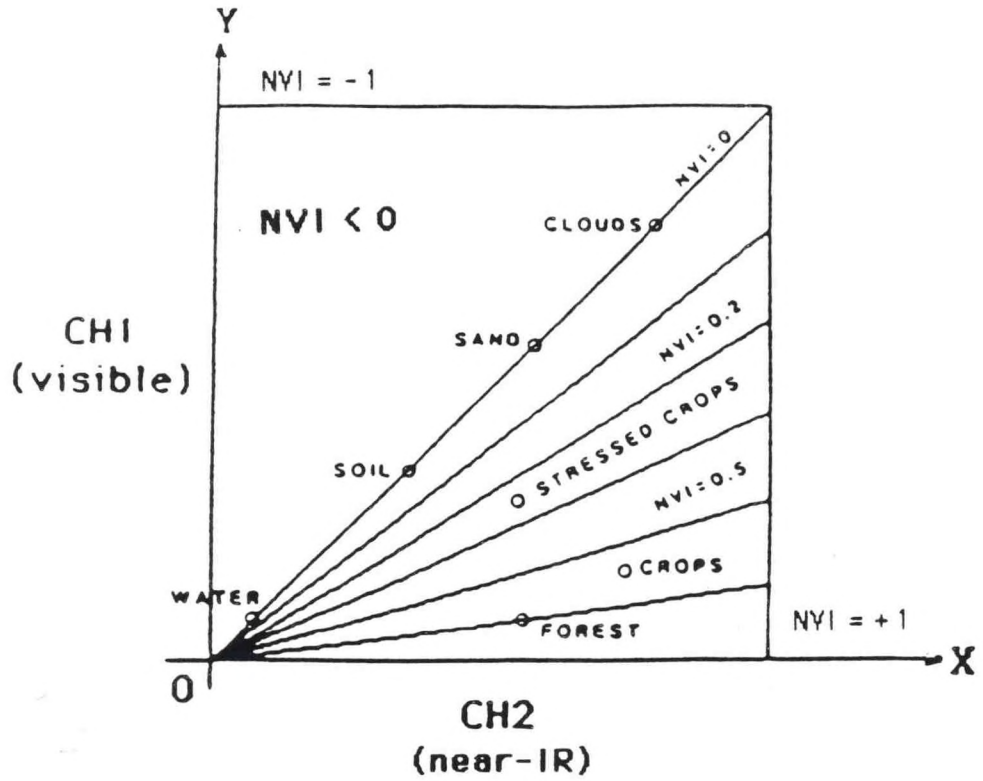

FIGURE 13. Surface features and clouds plotted as a function of the visible reflectance (AVHRR Channel 1), near-infrared reflectance (AVHRR Channel 2), and NVI. Source: Ambroziak, 1986.

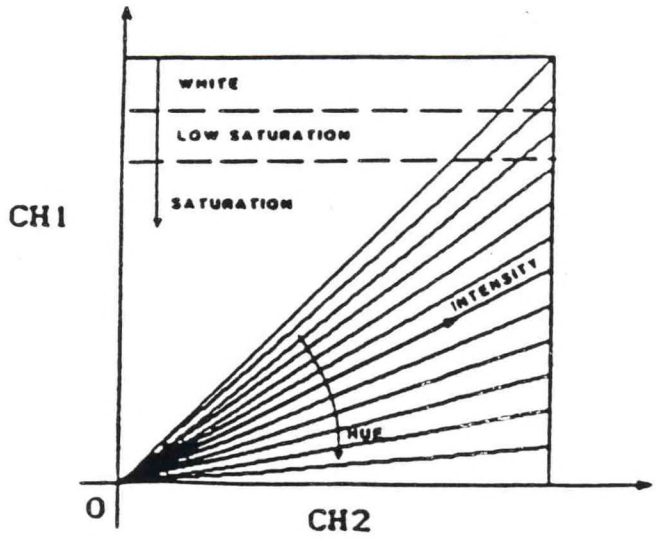

FIGURE 14. The mapping of hue, intensity and saturation. Source: Ambroziak, 1986.

completely block the longwave emission of the ground below them) produce a lower saturated version of the hue of the surface features. This gives the impression of looking through a thin cloud at the ground below.

Intensity is used to make distinctions among pixels with the same NVI. The maximum of the visible and near-infrared reflectances is mapped into intensity so that the higher this maximum value, the brighter the image. If an NVI value of 0.0 is displayed as red, various features with an NVI of 0.0 will be shown with different intensities of red. Water (NVI near 0.0, very low visible and near-infrared reflectances) appears black; bare wet soil (NVI near 0.0 with somewhat greater reflectances than water) is a pale dark red; dry soil and sand (NVI near 0.0 with still greater reflectances) are a medium bright red; and clouds (NVI near 0.0 with higher reflectances) appear as a bright red. Depending on how the saturation filter is set, some of the features with high visible reflectances will become white on the display. Forests generally are displayed with a lower intensity (darker shade) of green or blue than cropland because of their reflectance characteristics. The ACCS used in the African assessments is labeled as ACCS2r, which assigns blue to an index value of 1, red to 0 and magenta from 0 to -1 (Figure 15).

The intensity (I) of a color is mapped to the maximum of the visible and near-infrared reflectance as a distance along the vertical axis from IMIN = 0 (black) to IMAX = 255 (white). Hue (H) is continuous, varying around the color hexcone from HMIN = 0 (blue), 42 (magenta), 84 (red), 126 (yellow), 148 (green), 210 (cyan), to HMAX 252 (blue) again, and defines the vegetation index. The saturation (S) is used as a cloud filter, based on cloud temperature, and is the distance from the intensity axis radially toward the surface of the hexcone. Lowest cloud temperature is mapped to SMIN = 0 (white) and highest temperature is SMAX = 255 (pure or deep rich hue, Figure 16).

Analysis of AVHRR images is performed using a personal computer image processor (PCIP) system. The PCIP software facilitates image display, zooming, the creation of different video color look-up tables, and image annotation. The look-up tables are created according to the ACCS Intensity-Hue-Saturation Color Model.

The current ACCS, as used on the PCIP, generally employs two of many possible color-coordinate systems, ACCS-2r and ACCS-2b. Usually, ACCS-2r is applied for regions with known sparse vegetation cover and ACCS-2b is used for dense vegetation cover. Because the maximum hue resolution on ACCS occurs between the red and green portions, the red-green portion of the coordinate system is generally positioned over vegetated areas.

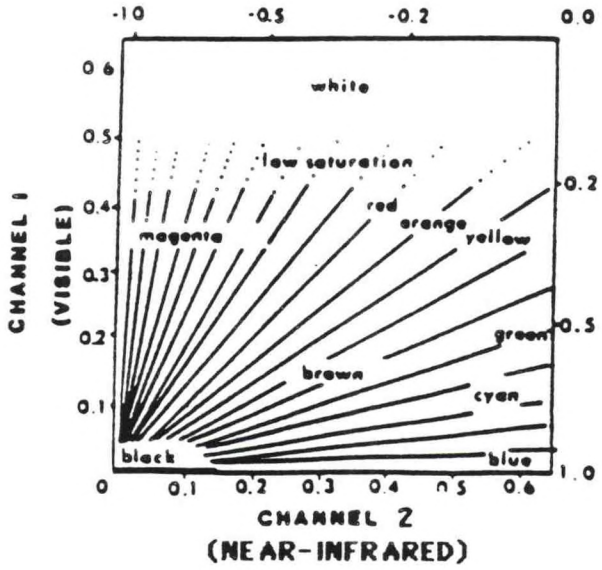

FIGURE 15. Ambroziak Color Coordinate System -- 2 cycle (ACCS2r). Source: Ambroziak, 1986.

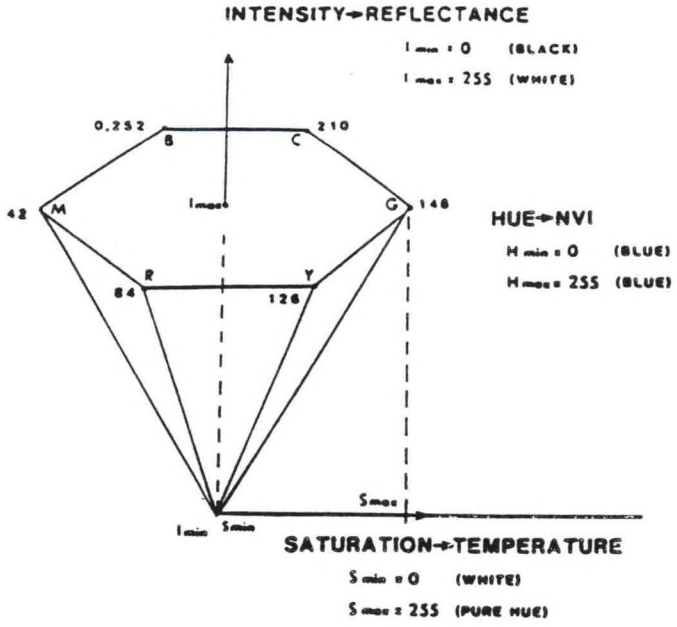

FIGURE 16. ACCS IHS color model. Source: Ambroziak, 1986.

2.4 REAL-TIME DATA ACQUISITION

Two systems are involved in the processing of satellite data. The first employs a VAX minicomputer to process the satellite data from computer tape to floppy diskette. The second, an IBM-compatible personal computer image processor (PCIP) system (Figure 17), is used to display and manipulate pre-processed images from diskettes (Figure 18).

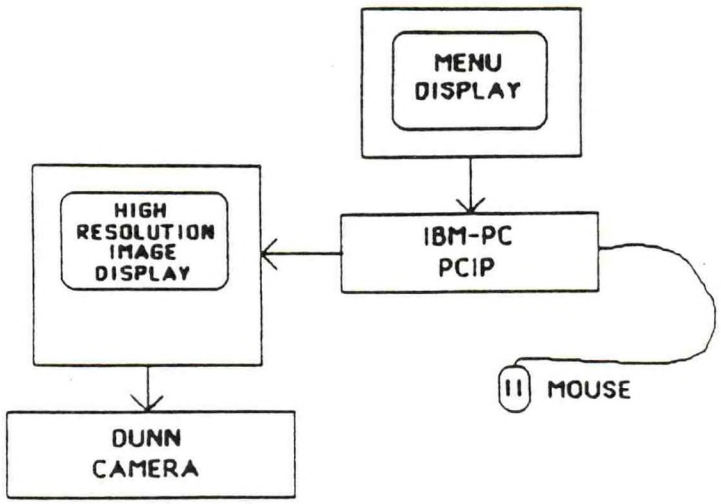

FIGURE 17. System configuration for PCIP (Personal Computer Image Processor).

A schematic overview of satellite data processing and output products is shown in Figure 19. Output products are provided in the form of satellite images using a high resolution video display monitor or photographs which capture display images. Other output products are NVI statistics and time series plots for defined geographical areas. These output products constitute one of the inputs to the operational agroclimatic assessment process.

The decision to use LAC, GAC or GVI data must be based on such considerations as data availability (historical and real-time), the task objectives, cost, available hardware, and time constraints. Generally it is less expensive to obtain GVI versus LAC or GAC, but information content may be compromised because of the sampling scheme. LAC resolution is most useful if an adequate number of acquisitions are available to develop cloud-free composites of the ground; this is particularly important in Africa, where cloud contamination is a serious problem.

LAC data can be acquired on a one-pass-per-week basis. This provides weekly coverage of the assessment area, but not in sufficient quantity to enable time compositing over 7-to-10 day periods for cloud-removal purposes. LAC data are used in the

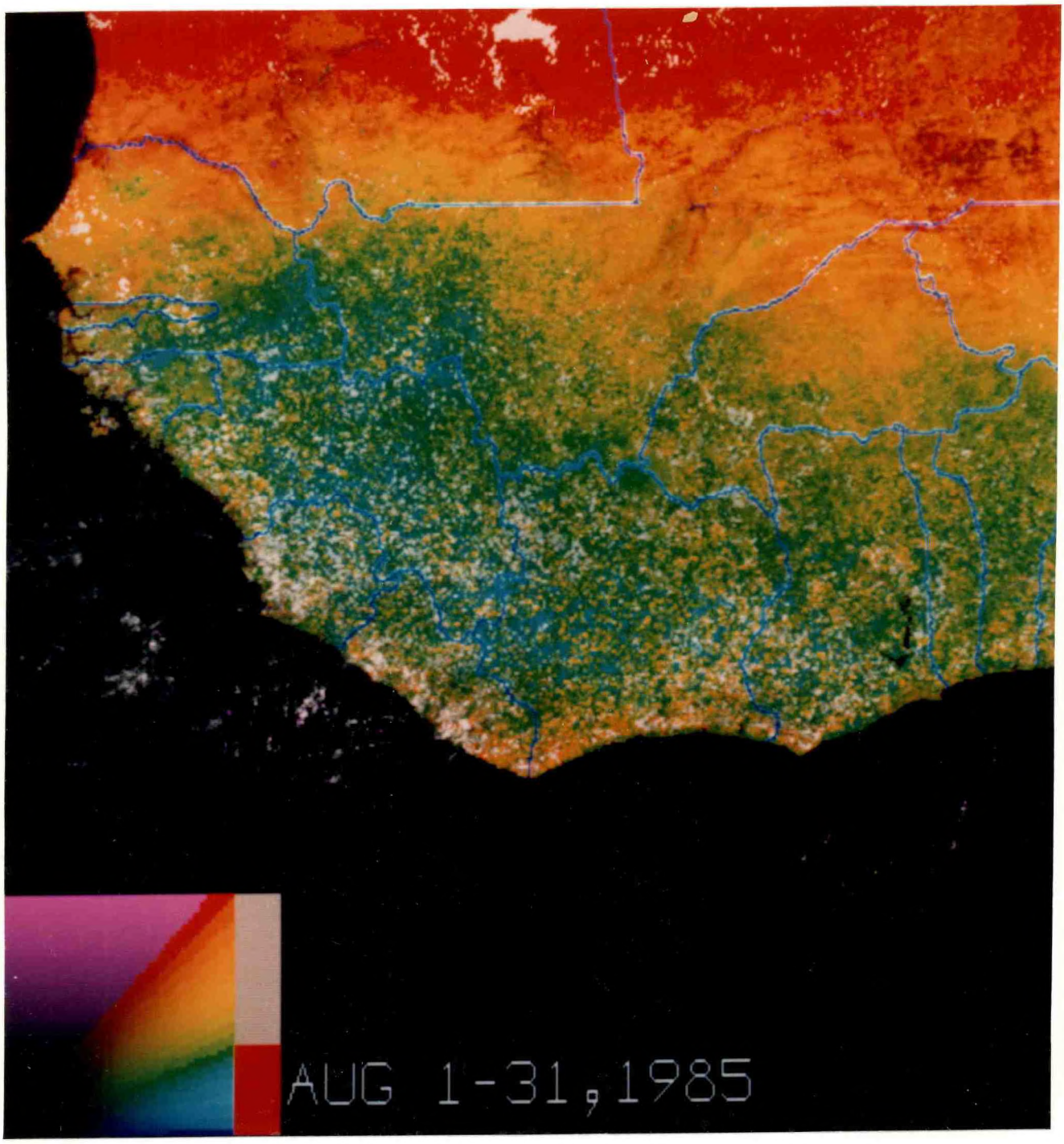

FIGURE 18. A composite ACCS image of West Africa produced by the PC image processor. The color scale is in the lower left. Biomass decreases as the hues progress from cyan (greenish-blue) through green, yellow, orange, and red. White areas are clouds.

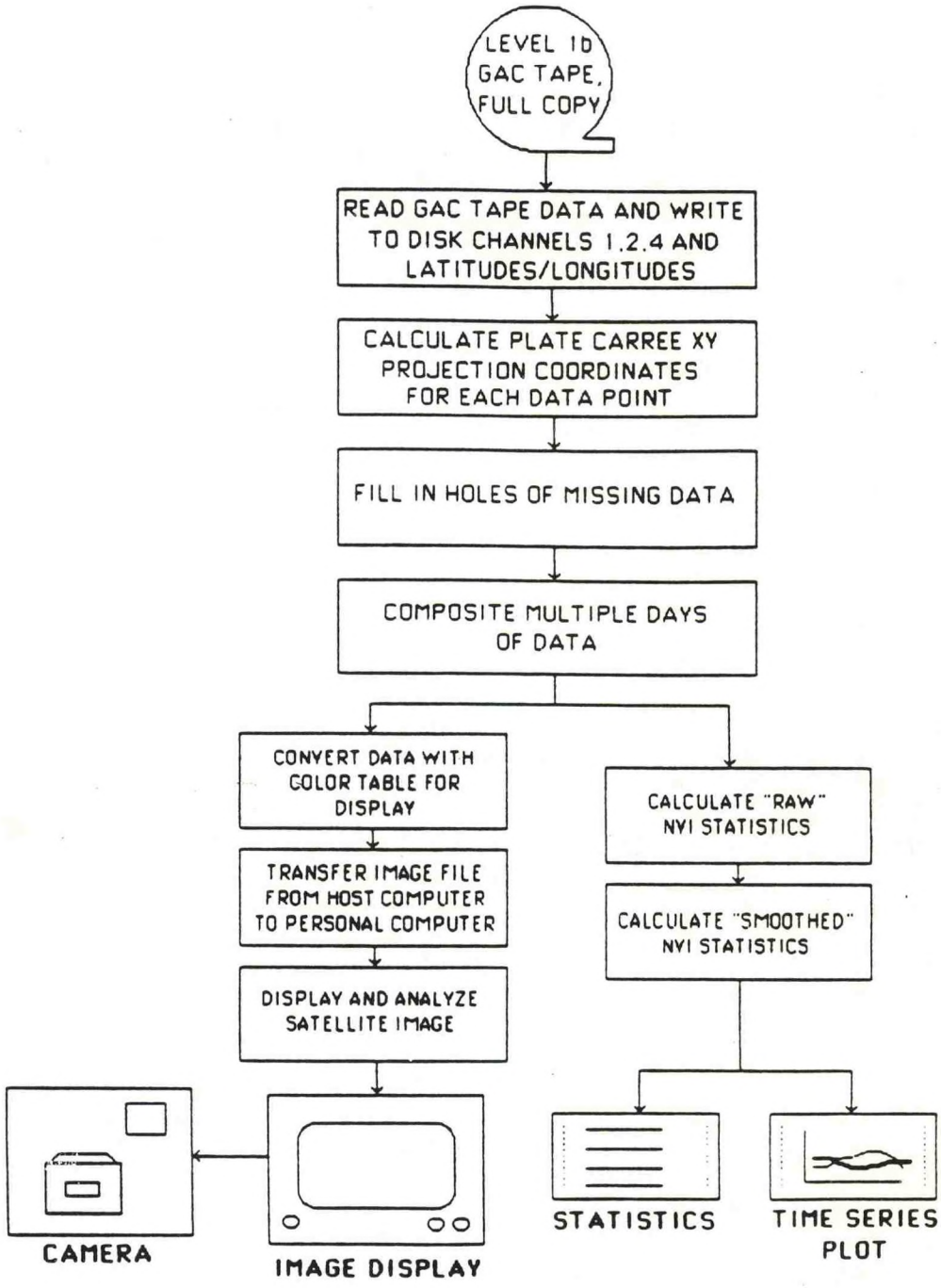

FIGURE 19. Overview of GAC data processing and output products.

interpretation of vegetation conditions when potential problem areas are identified either by interpretation of the GAC data or by information from one of the other assessment subsystems.

GAC resolution data were selected as the principal resource for large area analysis. GAC data available for the entire globe are acquired daily from NOAA/NESDIS and composited over 10-day periods to screen clouds and to compensate for atmospheric effects introduced by extreme scan angles, haze, and sub-pixel cloud contamination. Compositing is accomplished by retaining the greenest pixel (as measured by the NVI) from each 10-day period.

For the Sahel/Horn zone of Africa, priority was placed on daily GAC satellite data coverage to remove clouds and minimize atmospheric noise. To ensure total ground coverage for each day across the entire African continent (Senegal to Somalia), AISC uses approximately 90 percent of the scan line from nadir. This represents a selection of 1000 km on the ground of scan-line data on each side of nadir.

2.5 PRINCIPLES OF DATA INTERPRETATION

2.5.1 Interpreting Imagery

AISC assessors use the PCIP system to display and interpret AVHRR imagery. As earlier discussed, the ACCS depicts the condition of vegetation by using colors designed to enhance the information content of the data. Different hues (red, orange, yellow, green, cyan, blue) differentiate vegetation and water from soil and clouds. These hues are a function of levels of the visible (Channel 1) and the near-infrared portions (Channel 2) of the reflected sunlight. The colors of the ACCS display a continuum of hue and intensity (brightness). Sharp boundaries on the image, appearing as easily detected changes in hue, indicate actual changes in surface vegetation.

In the ACCS, the vegetation index is mapped by hue. Pixels with a different vegetation index value have a different hue so that healthy vegetation is green, stressed vegetation is yellow, and clouds are white. Intensity is controlled by the maximum value of both channels. Pixels with the same vegetation index and different Channel 1 and 2 values can be distinguished so that crops are light green and deciduous forest is dark green. Saturation is reduced to zero for the very high visible brightness values and thereby becomes a cloud filter. The presence of thin clouds or haze in an image is discerned as a reduction in saturation. Quantitative hue and intensity changes due to atmospheric conditions are partly compensated for by the qualitative perception of the human interpreter. The colors can be generally interpreted as illustrated in Table 2.

TABLE 2. Interpretation of land cover based on hue and intensity of colored images.

HUE	INTENSITY	
	Dark	Bright
red	wet or dark soil*	sand or low clouds
yellow	emerging or sparse plant cover over wet or dark soil*	emerging or sparse plant cover over sand or under scattered clouds
green	very healthy plants combined with standing water or forest	healthy field crops or similar plants
cyan#	dense forest	dense forests, maize or rice cover
magenta+	clear shallow or slightly turbid water	highly turbid, shallow, or partially cloud-covered water
COLORS WITHOUT HUE		
black	clear deep water or dark shadow	
white	clouds, snow, or colder high terrain	

*Dark reds, oranges, and yellows are shades of brown.
#greenish-blue
+purplish-red

It is important to recognize that the satellite imagery must be used in conjunction with other data including vegetation index values and station rainfall reports. Low greenness values may be due to cloud contamination which can be visually observed from the composited imagery, thereby qualifying the interpretation of the greenness index in terms of the vigor of the vegetation. The ACCS is, therefore, an analytical tool for qualitative assessment of greenness.

2.5.2 Vegetation/Biomass Index

In addition to the imagery, AVHRR Channel 1 (visible) and Channel 2 (near-infrared) data are used to produce the Normalized Vegetation Index for each pixel, i.e., a greenness index. Vegetation indices are designed to describe vegetation condition. These indices condense spectral information, discriminate vegetation from nonvegetation, and uniformly characterize crop conditions over a very large range of agricultural, seasonal and meteorological conditions. In principle, a vegetation index is a ratio or a difference of reflectance values in the near-infrared and the visible region of the spectrum. Remotely-sensed features

that have greater visible reflectance values compared to near-infrared (e.g., clouds, water, snow) will have low or negative vegetation index values compared to vegetation index values for green vegetation.

There are several advantages to using vegetation indices. Because the vegetation index is calculated using data from more than one channel, its value represents considerable data compression. In addition, these indices may compensate for variation in solar irradiance. They also partially correct for atmospheric path effects and reflectance differences of objects attributed to changes in the scan angle of the sensor. An ideal vegetation index should be sensitive to vegetation, insensitive to soil background, and uninfluenced by atmospheric path radiance.

Studies by van Dijk (1986) have shown that changes in scan angle, atmospheric moisture content, and pollutants can produce highly variable NVIs when calculated from daily data for a single pixel. Much of this variability (or noise) can be removed by compositing cloud-free pixels and spatially averaging NVIs over assessment regions. Specifically, the total set of the greenest pixels which have been cloud screened in a composited 50 km x 100 km assessment polygon (e.g., 1/2° latitude by 1° longitude) are averaged each week and assembled to provide an NVI time-series for the assessment polygon.

The variability in the NVI time-series based on regionally-averaged, weekly-composited data is also high, but not as great as with the daily data. To reduce this variability, but retain significant agricultural and environmental signals, weekly time-series for each grid cell are further smoothed by using a smoothing algorithm (van Dijk, 1986; van Dijk et al., 1987). The smoothing process depicts discernable NVI time-series differences (Figure 20). At key times during the crop-growing season, the spatially-averaged and temporally-smoothed NVI data are also mapped for year-to-year comparative analysis. This time-series approach is particularly useful if several years of AVHRR data are available.

2.5.3 Crop Condition Assessment

The color satellite images provide an overview of the surface vegetation/biomass conditions and are used to integrate and interpolate other data sets. NOAA satellite-derived vegetation/biomass indices are used to qualitatively assess crop vigor during the growing season. Both color images and vegetation indices are used to compare the current year with the previous years. Integrated analyses based on these NOAA satellite and weather station data are used to assess crop and rangeland conditions.

NOAA AVHRR data have significantly improved the reliability and spatial resolution of techniques for drought detection and

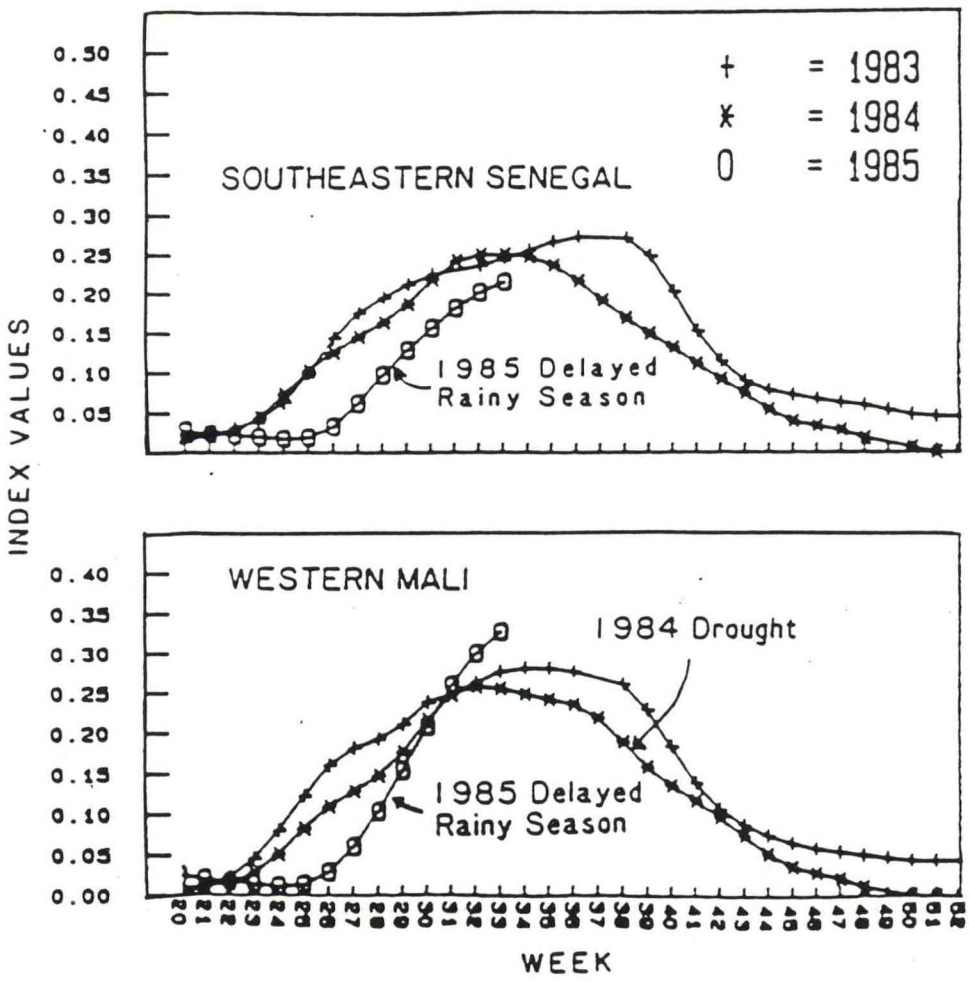

FIGURE 20. Smoothed Normalized Vegetation Index (NVI) curves for southeastern Senegal and western Mali. The graphs portray the 1983 and 1984 growing seasons, as well as the beginning of the 1985 season. Vegetation growth lagged considerably in 1985 due to delayed rains, but growth caught up with the prior years' levels by week 31 in western Mali. As of week 33, growth was still below prior years' levels in southeastern Senegal.

crop condition assessment. The signals for a disastrous drought year such as 1984 or a good crop season such as 1985 or 1986 are quite distinct (Figure 20). The integrated use of AVHRR imagery, vegetation-index time-series, and agroclimatic crop water balance models provides the methodology for detecting and assessing these strong signals.

2.5.4 NVI Crop Model

The vegetation index indirectly measures the amount of photosynthetically active phytomass. The vegetation index reaches its maximum value at about the beginning of the reproductive stage of crops (van Dijk, 1986). The decline in vegetation index starts during the reproductive stage when the crop accumulates the largest portion (50 percent) of its dry matter. When 90 percent of reproductive dry matter has been accumulated by the plant, the vegetation index has declined to less than half of its maximum value during heading. Temporal coverage is, therefore, an important determinant of the relation between biomass and yield. In particular, the NVI, depicting relative crop vigor at the critical growth period (i.e., flowering and reproduction), can be used as a yield indicator.

There is a close relationship between the reflectance of crop canopies and the estimated photosynthetically active phytomass in the form of Leaf Area Index (LAI), percent of ground cover, dry or fresh phytomass, and chlorophyll content. Vegetation indices have been used to estimate the amount of biomass (Prince and Tucker, 1986). In the case of forage, yield is nothing but biomass; there is a strong relationship between yield and spectrally-derived information on biomass, LAI, percent cover, and maximum greenness. However, for grain crops, spectrally derived estimates are generally not as good.

Accurate prediction of the effect of stress on crop yields requires knowledge of the calendar days on which a crop reaches certain development stages. The most promising tool for estimating crop stage dates is a time-series of NVI. It is constructed using the reflectance data of the same area collected on different dates.

The relationship between the NVI and the yield of the cereal is of utmost interest. The NVI at the time of heading seems to provide the best indication of yield: the greater the NVI, the greater the yield. After heading, when the leaves senesce, the relationship between vegetation index and yield starts to decline.

African agricultural practices are characterized by shifting cultivation with long fallow periods, partial clearing and burning of fallow land, little or no fertilizer, limited or no weed control, multicrop and multihybrid crop systems, low technical input, and small and irregularly bordered fields. The fields are scattered across a vast expanse of rough bush. Crops make only a small contribution to the total vegetation index of

the area and the NVI profile therefore represents an index of the greening for the vegetation of the entire area. Consequently, the conditions of a single crop with its varied cultural practices can be monitored only indirectly. Therefore, it is assumed that abnormal conditions will affect development of all of the vegetation in the area. The effect of growing conditions on a single crop is derived indirectly using the vegetation index data along with additional information such as crop calendar, precipitation and land use. Unfavorable weather during the reproductive phase of a crop should result in a low vegetation index for the area and consequently a low crop yield.

Determining the timing of the reproductive phase of the crops is critical to this approach. For 80-day millet the critical phase of its reproduction will be seven weeks after spectral emergence (NVI begins increasing). For 100-day sorghum this will be nine weeks and for 110-day groundnuts, twelve weeks.

After the selection of the critical period for a specific crop the NVI values for that week are regressed against historical yield. Figures 21 and 22 illustrate a regression model for sorghum and millet. A predicted yield is calculated using the NVI value from the ninth week after green-up for sorghum; for millet, the seventh week after spectral emergence was considered to be the critical week.

The comparison of the observed versus the predicted sorghum yields for selected regions in the Sahel is shown in Figure 23. The results suggest this method of estimating sorghum and millet yield from NOAA AVHRR data has considerable potential.

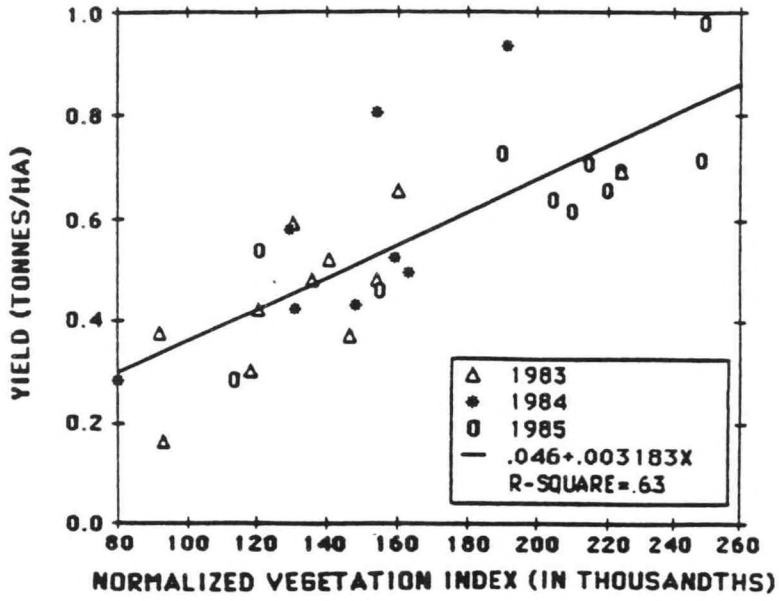

FIGURE 21. Observed sorghum yield versus NVI for the administrative departments of Burkina Faso, 1983-1985.

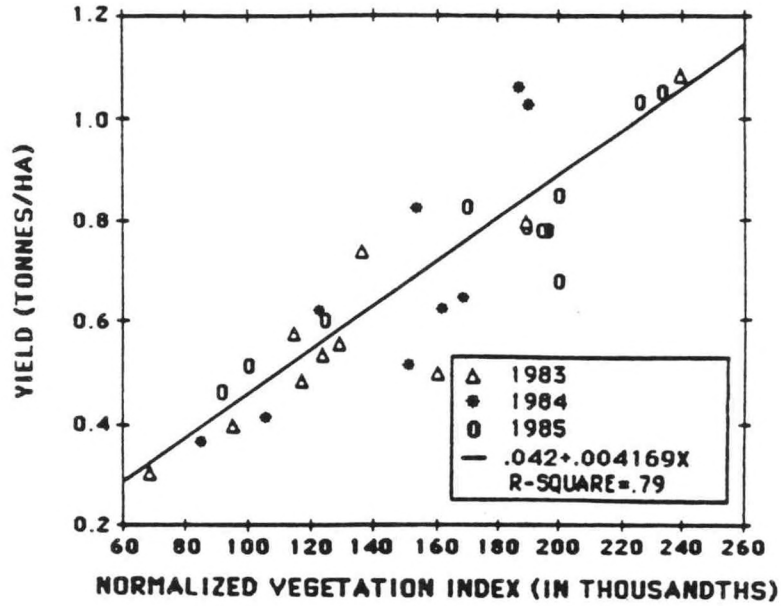

FIGURE 22. Observed millet yield versus NVI for the administrative departments of Burkina Faso, 1983-1985.

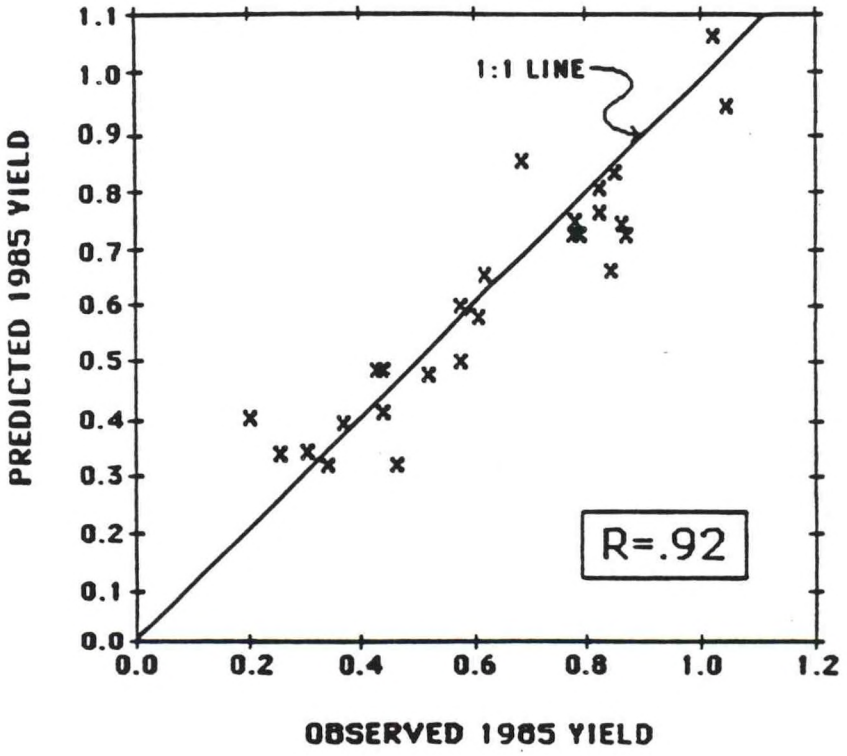

FIGURE 23. Predicted versus observed sorghum yields in selected regions of the Sahel, 1985. The NVI model used in this test was derived from 1983 and 1984 data.

3. WATER BALANCE INDEX

Decadal rainfall data serve as a primary input to a soil moisture budget and crop condition index based on methodology developed at the U.N. Food and Agricultural Organization (FAO) and referred to as the "FAO index" (Frere and Popov, 1979; FAO, 1986). The objective of this approach is to account for physical and biological conditions affecting the moisture status of a given crop, and integrate them over the course of crop development.

Computations are initiated at the beginning of the cropping season, which may be defined by normal agronomic practices, first occurrence of 30 mm of rainfall in a decade, onset of rainfall one-half the potential evapotranspiration (PET) rate, or as selected by the assessor. Normal PET has been estimated for all stations by AISC using the Penman method (Penman, 1948). Crop water requirements are calculated using the PET rate and crop coefficients which are based on crop phenology starting from planting time. These coefficients are derived from the work of Doorenbos and Pruitt (1977). Rainfall in excess of crop water requirements is accumulated as soil water reserves, and as long as these reserves remain between zero and the soil water storage capacity (based on soil type and crop), no adverse affect on crop yields is indicated. The water balance index is set to 100 at planting time (no moisture problems during that decade; yield prospects excellent). In any subsequent decade, if the soil water reserves exceed the soil water storage capacity (surplus of water) or decrease to zero (deficit of water), the water balance index is reduced. At any time during the crop growing cycle, the index indicates what percentage of the total crop water requirements were met during the cumulative period. The computations must be carried through to crop maturity to obtain index numbers for use in the final estimates of crop yields.

Operationally, the index is computed for many stations in the Sahel and Horn of Africa countries. Table 3 illustrates a sample work sheet for the water balance index at Dori, Burkina Faso. Three outputs from the computations are reviewed in the assessment process: soil water reserves, surplus or deficit of water, and the water balance index itself. These parameters can be analyzed as time-series for individual stations, or they may be plotted on a map (Figure 24) for spatial analysis.

In spite of the physically-based nature of the computations, use of the results in crop condition and yield assessments should include consideration of local conditions. Resulting index values can be compared with values in recent years when crop yields were known. Furthermore, with a long historical 10-day rainfall data series such as that of the AGRHYMET System, normal index values and percentile rankings of individual years can be calculated, providing a much better perspective.

The FAO index was developed primarily for use in the Sahel, but it has also been applied to rain-fed crops in Asia.

TABLE 3. 1978 cumulative water balance index for Dori, Burkina Faso (modified after Frere and Popov, 1979). The numbers 1, 2, and 3 indicate the first, second, and third decades of the month.

	MAY			JUN			JUL			AUG			SEP			OCT		
	1	2	3	1	2	3	1	2	3	1	2	3	1	2	3	1	2	3
P_N	7	9	10	14	20	25	49	50	52	63	65	61	40	32	24	10	4	1
P_A	4	11	14	23	18	58	51	48	134	9	29	28	15	32	6	0	3	
PET	75	78	80	68	63	59	59	57	59	48	47	50	47	50	52	55	59	59
KC						0.3	0.4	0.5	0.8	1.0	1.0	1.0	0.6	0.5				
WR						18	24	29	47	48	47	50	28	25		Σ WR=316		
P_A-WR						40	27	19	87	-39	-18	-22	-13	7				
R_S						40	60	60	60	21	3	0	0	7				
S/D						0	7	19	87	0	0	-19	-13	0				
I						100	100	100	100	100	100	94	90	90				

P_N = normal rainfall (mm)

P_A = actual rainfall (mm)

PET = normal potential evapotranspiration (mm)

KC = crop coefficient

WR = PET * KC = water requirement (mm)

P_A - WR = difference between rainfall and water requirements

R_S = soil water reserve

S/D = surplus / deficit

I = Water Balance Index

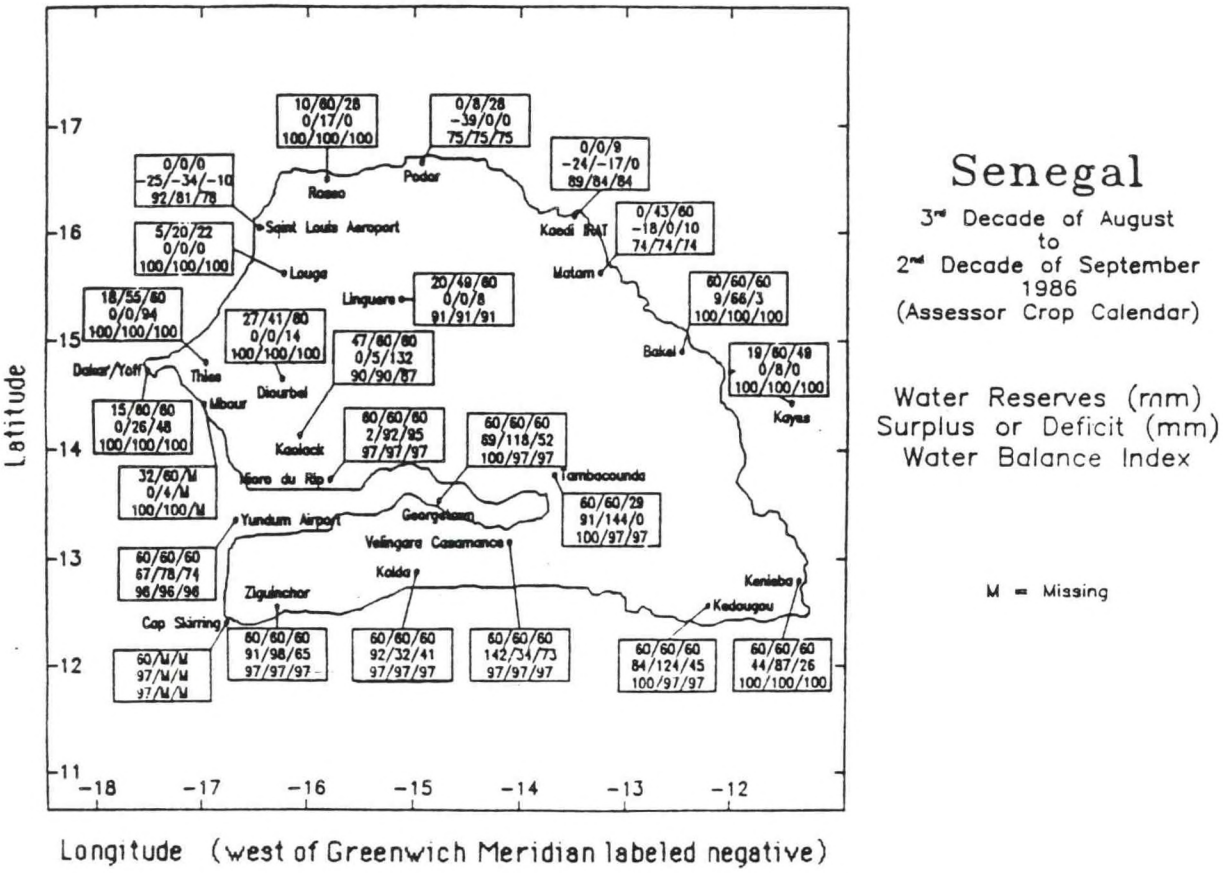

FIGURE 24. Water reserves, surplus, and water balance index, Senegal, 1986.

Comparison with independent data has shown the index to be relatively insensitive to high moisture levels, but it appears to indicate extreme drought conditions well. Use of the index for quantitative estimates of crop yields has produced mixed results. Nevertheless, the incorporation of additional parameters in this approach gives it an added dimension, and with refinement and improvement it should eventually prove superior to using rainfall data alone.

4. STATISTICAL CROP MODELS

4.1 PRECIPITATION CROP MODELS

Possible relationships between rainfall and yield were investigated using agricultural statistics for administrative regions (Kaylen, 1986; Kaylen and Le Duc, 1988). The goal was to provide a quantitative input into the evaluation of weather-related impacts on crop yields in the Sahel. Yield data for the most recent five years provided the basis for the models, with additional data from earlier years also available for model development in most countries. The quality and representativeness of these data were unknown but many sources of problems had been identified. For example, it was recognized that reporting procedures over the period of years might have been inconsistent. But for model development it was necessary to assume that these samples were all from the same population. Outliers were eliminated on a case-by-case analysis.

4.1.1 Statistical Model

Given the lack of good-quality data, the limited years of data which are available, the existence of information on only one independent variable (precipitation), and the large number of models to calculate, the model had to be a simple one.

The statistical model for a particular crop and region was of the form:

$$Y_t = B_0 + B_1 X_t + e_t$$

where Y_t is the yield for year t in metric tons per hectare

B_0 is the intercept term

B_1 is the coefficient for the independent variable, X_t

X_t is cumulative precipitation for year t in millimeters

e_t is the stochastic error term

A simple linear regression model was chosen as the appropriate form for modeling. Plots of rainfall versus yield for most regions and crops demonstrated a positive and linear relationship between yield and rainfall. It can be assumed that at some point a positive, linear relationship will cease to hold. However, in the Sahel, rainfall is rarely so great that yields do not respond in a positive linear fashion.

4.1.2 Model Specification

The models were formulated with the aid of a computer. For each model, regression statistics, correlation coefficients, a graph of the actual and predicted yields, and a plot of rainfall versus yield were obtained. Regions within a country could be

modeled individually or in groups of up to five.

When selecting rainfall stations, the aim was to choose stations that represented different climatic regimes within a region. Because the climatic regimes followed a north-south pattern, stations were selected in a north-south distribution. Not all regions have sufficient stations within their boundaries, so other stations located in the same climatic regime were selected. The meteorological data were examined for each station to determine if the time periods corresponded to the same years as the yield data. If years were missing, the station was usually not used. The rainfall for each station was weighted such that the sum of the weights equaled 1.0. Stations representing areas where more crops were grown received proportionately higher weights.

The next step was to determine if the rainfall data from the stations selected by geographic location had a good fit to the yield data. The fit was determined by calculating the correlation between precipitation and yield for the following combinations of months (6 = June, 7 = July, etc.):

6	6+7	6+7+8	6+7+8+9
	7	7+8	7+8+9
		8	8+9
			9

If the correlation coefficients were not sufficiently great (generally over at least .40) then correlation coefficients were calculated for each station individually to determine if the aggregate data were affected by one station. Once stations were selected and any adjustments from the original selection noted, the months used for the August and September models were identified.

Potential months to include in a particular model were determined by finding the time period when rainfall was most critical to plant development. The period of time differs between regions, crops, and varieties of a single crop. Agronomic information on planting dates, lengths of plant development, and critical periods within the development cycle were used to identify reasonable months. Given this information, the correlation coefficients for the critical period were calculated. The highest correlation coefficient that corresponded to a reasonable month or accumulation of months was then chosen as the X_t variable for the model.

As an example, see Table 4. June through August would be in the August model and June through September in the September model.

TABLE 4. Cumulative precipitation versus yield correlation coefficients for millet in Bougouriba, Burkina Faso. Period of record is 1979-85.

Period	June	July	August	September
June	0.5799	0.6049	0.8334	0.8287
July		0.3647	0.7223	0.6394
August			0.5116	0.4607
September				0.4607

Model performance was further improved by again checking for outlying years for the model under consideration. The years to eliminate were determined by plotting yield against precipitation for the months selected in X_t. Years where yield was more than two standard deviations from the average were eliminated.

Finally the regression model was run to determine the constants B_0 and B_1. Models with an R^2 of less than .25 were labeled not usable. With an R^2 of less than .50 they were considered questionable. A low R^2 could be attributed to poor-quality data or to the effect of factors other than cumulative rainfall on yields. Such other factors might include technical inputs like fertilizer and management practices or natural events like insects and disease or rainfall distribution within a month.

The coefficients of acceptable models were then entered on a microcomputer spreadsheet program. The current year's rainfall data were entered to calculate yield estimates for the current growing season.

Finally, a plot of the actual and predicted yield values was used to determine model performance visually. For example, referring to Figure 25, the regression model picked up the direction of change and most of the magnitude.

Two models were selected: the "best" model using only precipitation through August (Model #1), and the "best" model using precipitation through September (Model #2). The 1986 forecasts from Model #1 (millet in Niger) in 1986 are shown in Table 5 under the column "AUG. EST."

4.2 OTHER MODELS

Several other models in a research and development stage are being evaluated or adapted for application. These models are for areas where one or more of the above models either does not exist or exists and is not reliable. The water balance index models, such as the FAO index, are being evaluated by AISC with respect to quantitative relationships with yield. Plant process models are being evaluated for application in small geographic areas and scenario analysis.

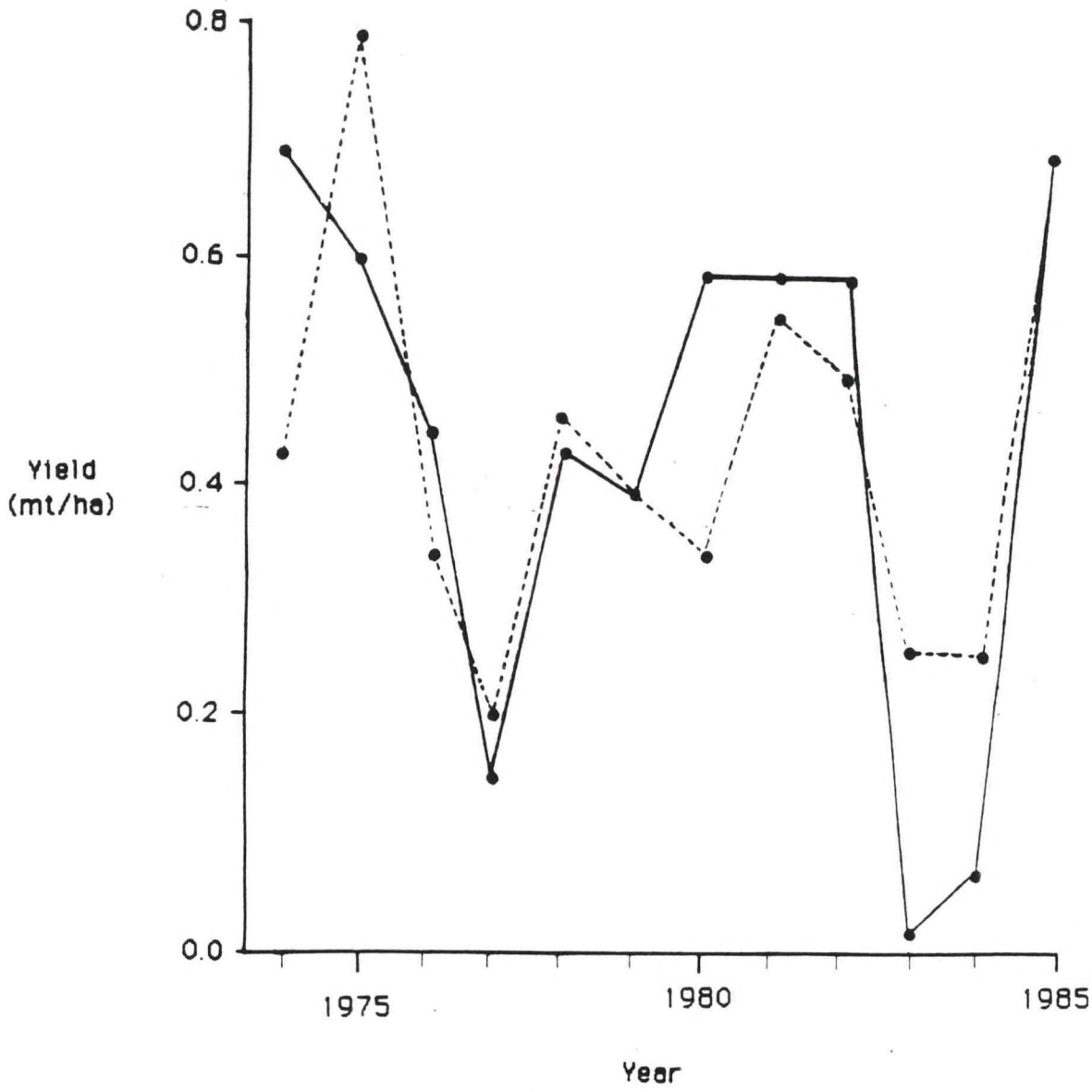

FIGURE 25. Combined millet/sorghum yield in Senegal. Solid line is yield reported by Senegal government; dashed line is projected yield based upon regression model. Source: Kaylen, 1986.

TABLE 5. Niger models. The statistical rainfall models for millet yield in Niger. These models incorporate monthly rainfall data through August ("AUGUST MODEL") for six administrative departments across Niger and were used to forecast 1986 yields. The forecast (AUG. EST.) is based on rainfall totals for the months listed under the AUGUST MODEL heading. The column headed R*R is the square of the correlation coefficient of the estimates based on data from 1979 through 1985. The actual yield forecasts released by NOAA/AISC also used the NVI models, water balance indices, and other available information.

REGION	STATION	WEIGHT (WT)	MODEL #1							
			AUGUST MODEL	PRECIP in mm. (PCP)	WT*PCP	B0	B1	X1	R*R	AUG. EST.
Diffa	N'Guigmi	0.333	6-8	102	33.966	-0.0169	0.0016	146.52	0.54	0.21
Diffa	Maine-Soroa	0.333	6-8	180	59.94					
Diffa	Goudoumaria	0.333	6-8	158	52.614					
Dosso	Gaya	0.333	7-8	452	150.516	0.24	0.0006	271.395	0.46	0.40
Dosso	Niamey Aeroport	0.333	7-8	202	67.266					
Dosso	Filingue	0.333	7-8	161	53.613					
Maradi	Maradi Aeroport	0.5	6-8	458	229	0.166	0.001	324	0.66	0.49
Maradi	Bouza	0.5	6-8	190	95					
Niamey	Niamey Aeroport	0.5	7-8	202	101	0.1426	0.001	181.5	0.56	5.32
Niamey	Filingue	0.5	7-8	161	80.5					
Tahoua	Tahoua	0.5	7-8	187	93.5	-0.0262	0.0024	223.5	0.86	0.51
Tahoua	Birni N'Konni	0.5	7-8	260	130					
Zinder	Zinder Aeroport	0.5	6-8	370	105	0.2762	0.0005	342.5	0.42	0.44
Zinder	Magaria	0.5	6-8	315	157.5					

PART III: THE END PRODUCT -- "PUTTING IT ALL TOGETHER"

The final objective of these activities is to arrive at a single assessment of crop condition or crop yield prospects using all of the diverse information which has been discussed. Each of the four types of analysis -- subjective rainfall, normalized vegetation index, water balance index, and statistical yield models -- can give an independent assessment of crop condition or crop yield. The final assessment might be the work of a single individual analyzing and weighing information from other members of the assessment team working at more basic levels, or each member might analyze one type of information to come up with an assessment independent of the others, the differences to be resolved by discussion. In either case, even though hard data have been used in rigorous models and objective analyses, the final assessment requires some degree of subjective judgment. Therefore, an assessor's experience influences the accuracy of the assessments.

Monitoring of crop conditions begins with daily routines; this entails at least a cursory review of weather maps and satellite photos, summarized in the form of notes. A more in-depth examination of conditions every ten days is summarized in another set of notes, and formalized as highlights of new developments. A complete analysis at the end of each month is more oriented toward yield potential in the form of a formal report, with supporting graphs, maps, and tables (see Figures 26, 27 and 28). Toward the end of the growing season, quantitative forecasts are made for crop yields in each administrative region of each country being monitored. Initial forecasts are issued at the beginning of September, and final forecasts are issued at the beginning of October. Table 6 shows a sample of the yield forecast information transmitted by cable to USAID missions in Africa at the end of the 1986 growing season.

TABLE 6. NOAA/AISC millet yield forecasts for Niger, issued in September 1986 (yields in mt/ha, areas in 1000s of hectares).

	MILLET					
ADMINI-STRATIVE REGION	1981-85 MEAN CROP YIELD	1981-85 MEAN CROP AREA	1984 REPORTED CROP YIELD	1985 REPORTED CROP YIELD	NOAA/AISC 1986 YIELD FORECAST	FORECAST AS % OF 1981-85 MEAN
Diffa	.32	44	.02	.48	.30	94
Dosso	.40	610	.27	.45	.38	95
Maradi	.40	636	.27	.48	.45	112
Niamey	.38	796	.25	.44	.32	84
Tahoua	.39	408	.23	.45	.51	131
Zinder	.43	596	.28	.48	.46	107

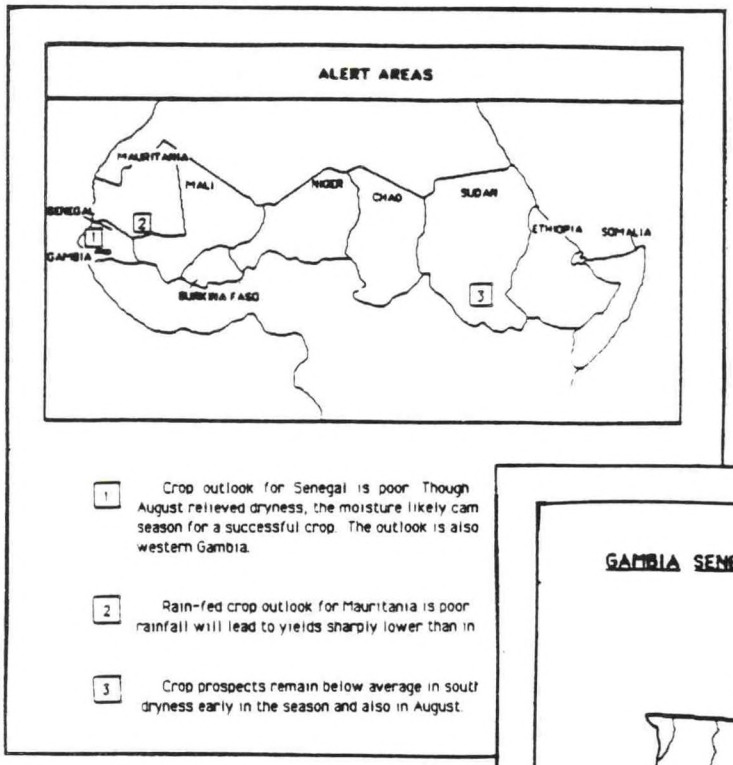

FIGURE 26a.

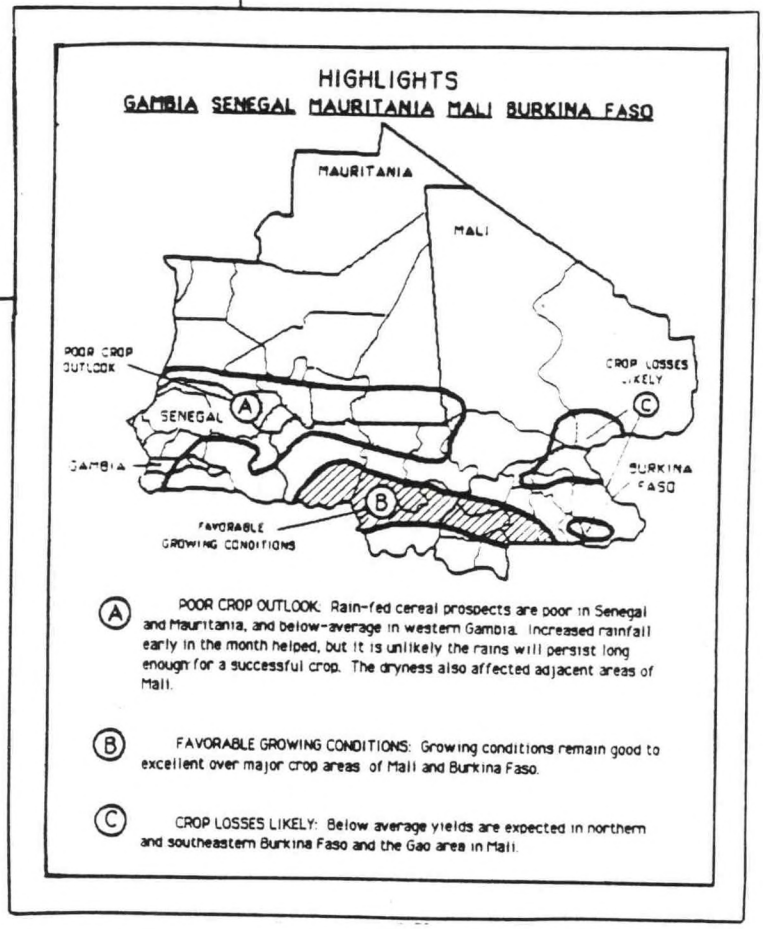

FIGURE 26b.

FIGURE 26. Sample pages from monthly assessment showing a) areas of interest and b) monthly highlights of regional conditions for Western Sahel.

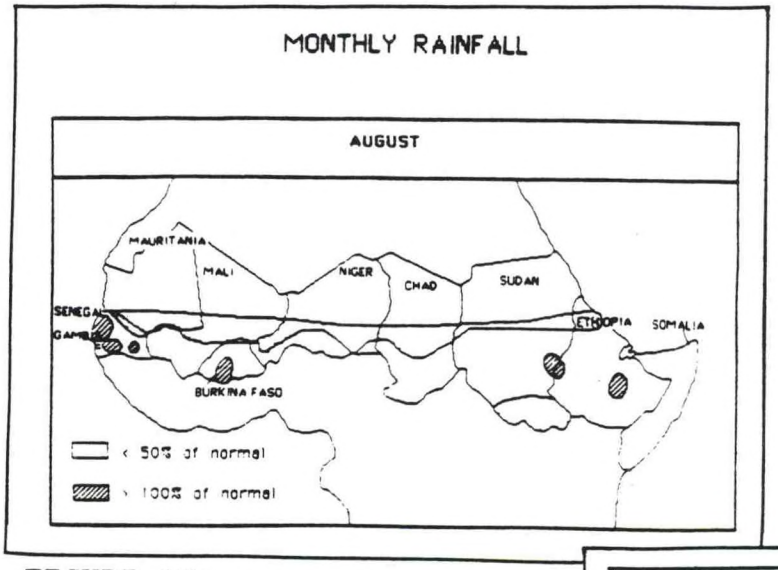

FIGURE 27a.

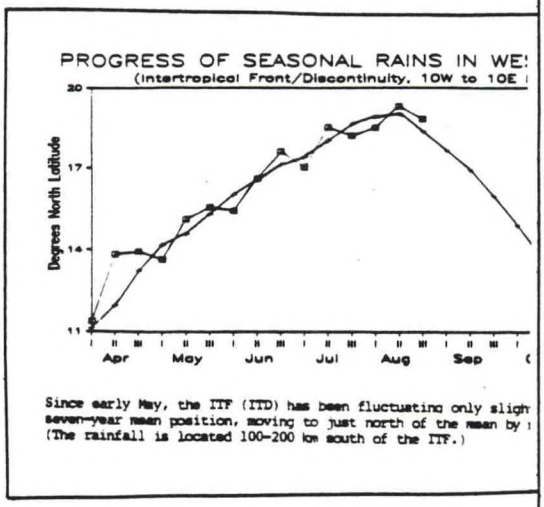

FIGURE 27b.

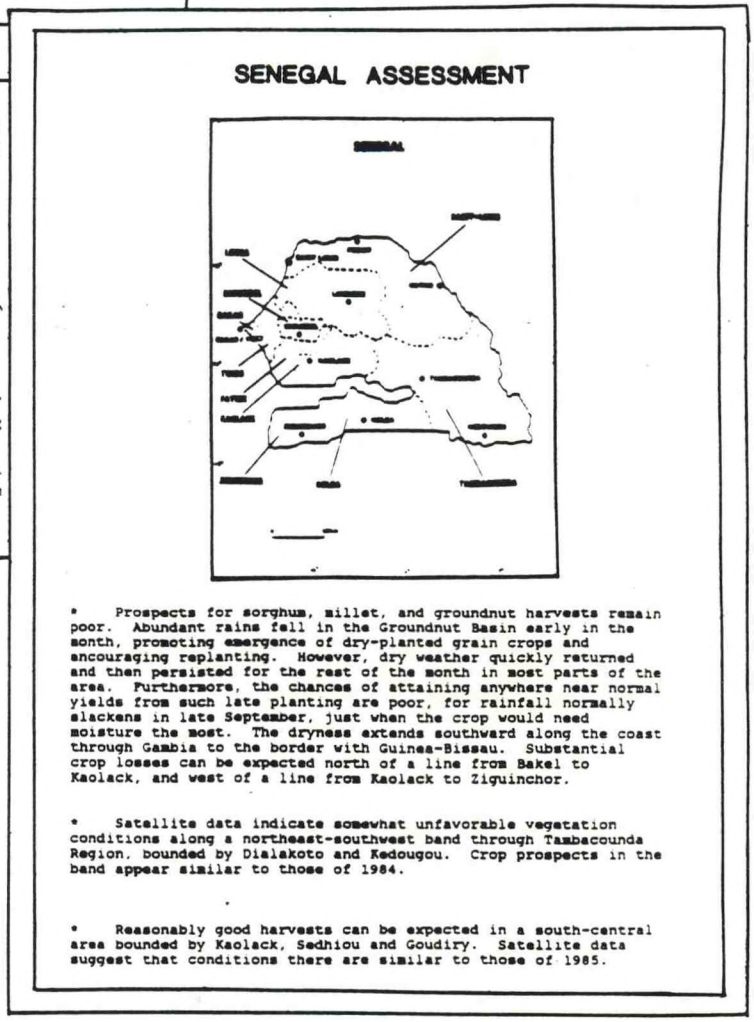

FIGURE 27c.

FIGURE 27. Sample figures from monthly assessment showing a) rainfall distribution, and b) the progress of the Intertropical Front, and c), sample page with monthly synopsis of conditions and their impacts.

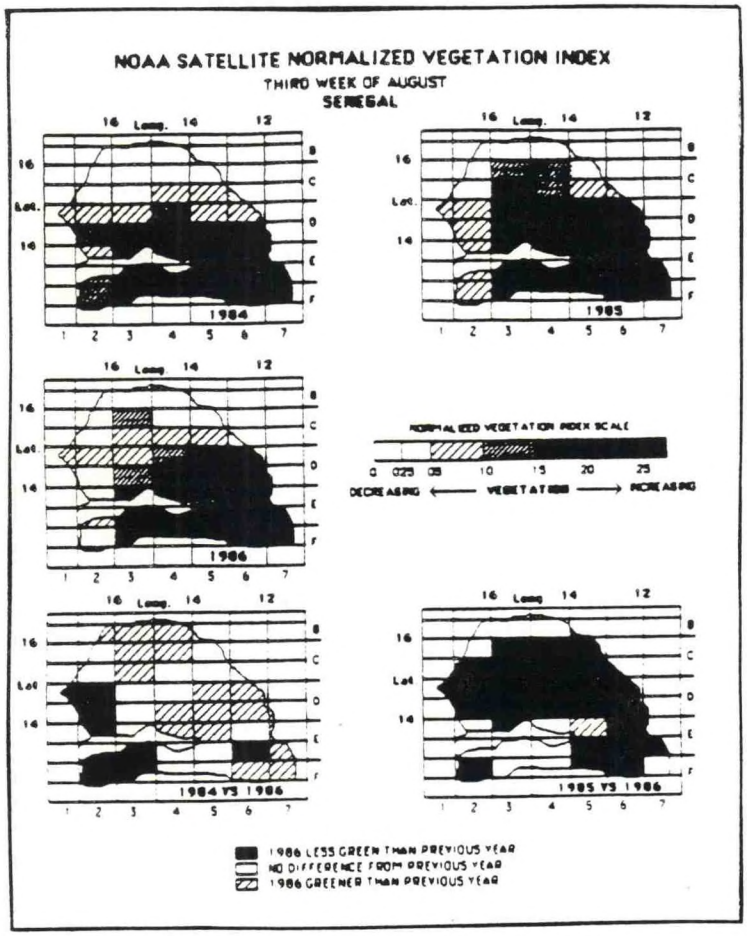

FIGURE 28a.

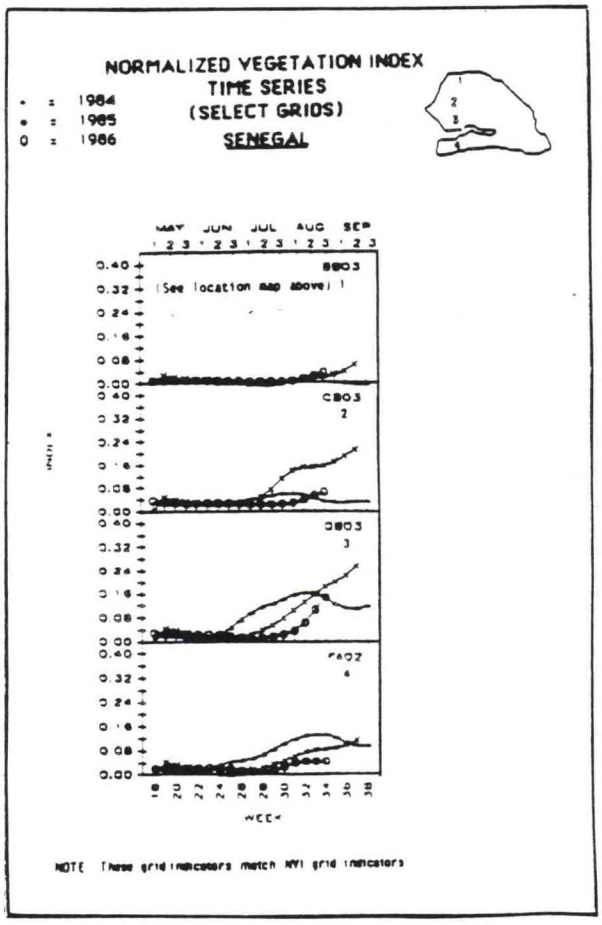

FIGURE 28b.

FIGURE 28. Sample pages on NVI data from monthly assessment, showing a) amount of greening in gridded-cell format, and b) time-series plot.

Merging of information in the assessment process must be accomplished smoothly. Final products from the analyses will be mostly in the form of maps and time-series, and the scales in time and space should be standardized for easy comprehension. The set of maps of background information and all of the basic and derived parameters can be overlaid as transparencies or on a light table in various combinations to compare results and make additional refinements.

None of the data can stand alone; they are given perspective by comparison with historical data. Long-term records of rainfall permit a rigorous analysis, but the moisture index and NVI are available only in recent years, and must therefore be compared with actual conditions (results) on a year-to-year basis.

The merging process illustrated in Figure 29 focuses on resolving inconsistencies in the results of the various analyses. It is essentially a search for convergence of information. Usually the results give similar indications, but sometimes differences must be traced back through the analyses to ascertain the validity of the results. In some cases, certain results might have to be rejected outright. It is a long and tedious process requiring careful attention to detail.

Preliminary and final AISC yield forecasts for Niger and Burkina Faso, as issued in 1985 and 1986, were compared to official yields for administrative regions reported following the harvest. Figures 30 and 31 show the NOAA yield forecasts versus the country yield reports for 1985 and 1986 respectively.

In general, AISC forecasted yields were less than the official country reports for many regions for the 1985 crop year. In 1986 this negative bias was no longer apparent in the millet forecasts, but was still slightly evident in the sorghum forecasts. Note that, in general, the scatter of the data was much less in 1986 than in 1985.

To make a quantitative comparison, the difference between the AISC forecast and the official report was calculated for each crop (millet and sorghum) and each region of the two countries. This comparison is summarized in Table 7 on page 60. In general, the differences in 1986 were about half of those in 1985, a substantial improvement in forecast accuracy. Note that in both years the AISC initial forecasts made in early September were nearly as accurate as the final forecasts issued in early October.

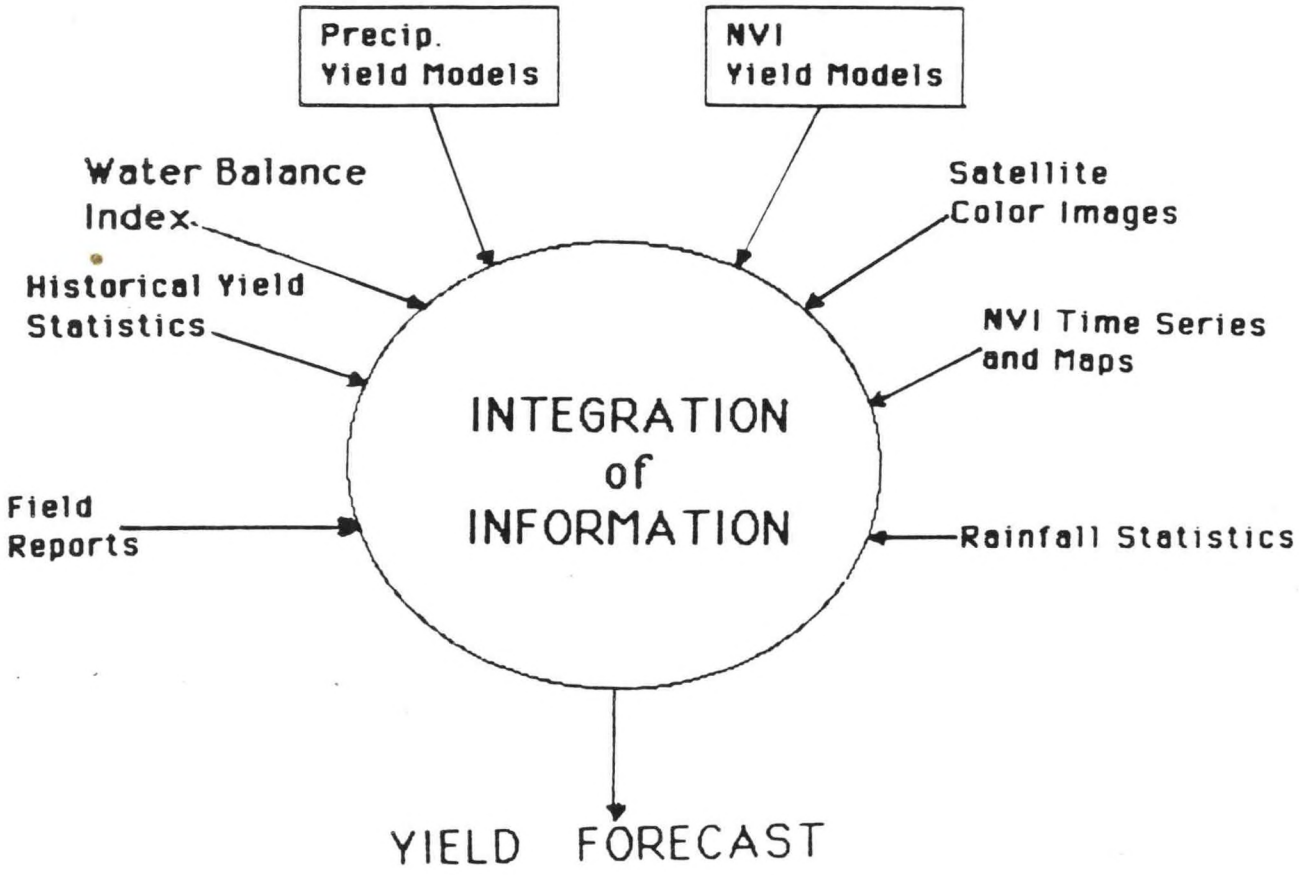

FIGURE 29. Schematic illustration of the final assessment process.

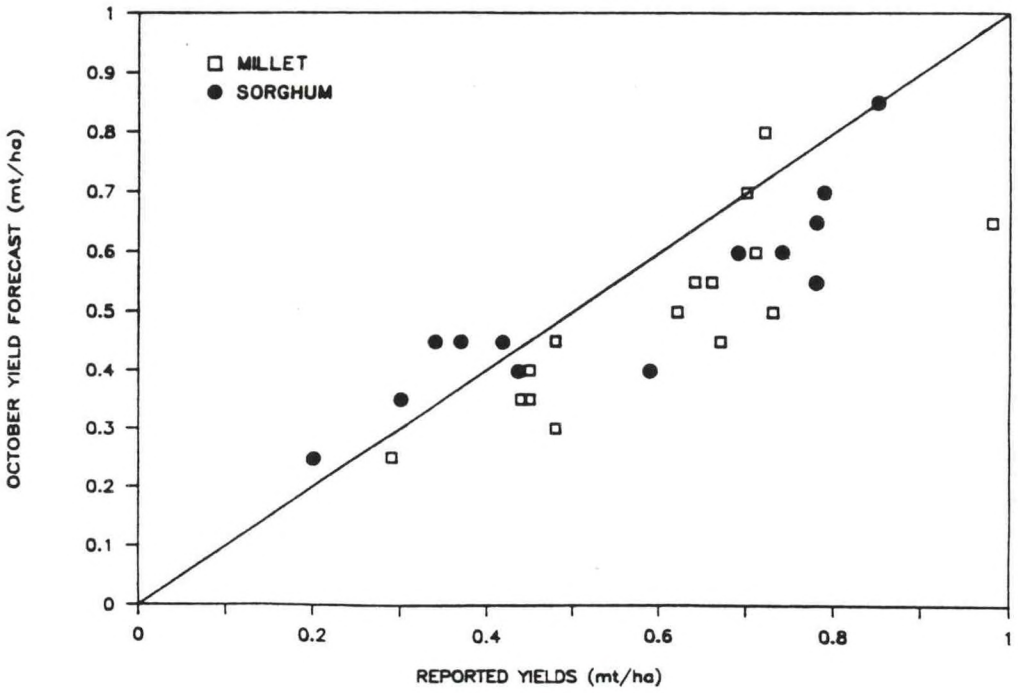

FIGURE 30. Comparison of NOAA/AISC October 1985 millet and sorghum yield forecasts with reported yields for the administrative regions of Niger and Burkina Faso. The diagonal line represents a perfect one-to-one fit between reported and forecasted yields.

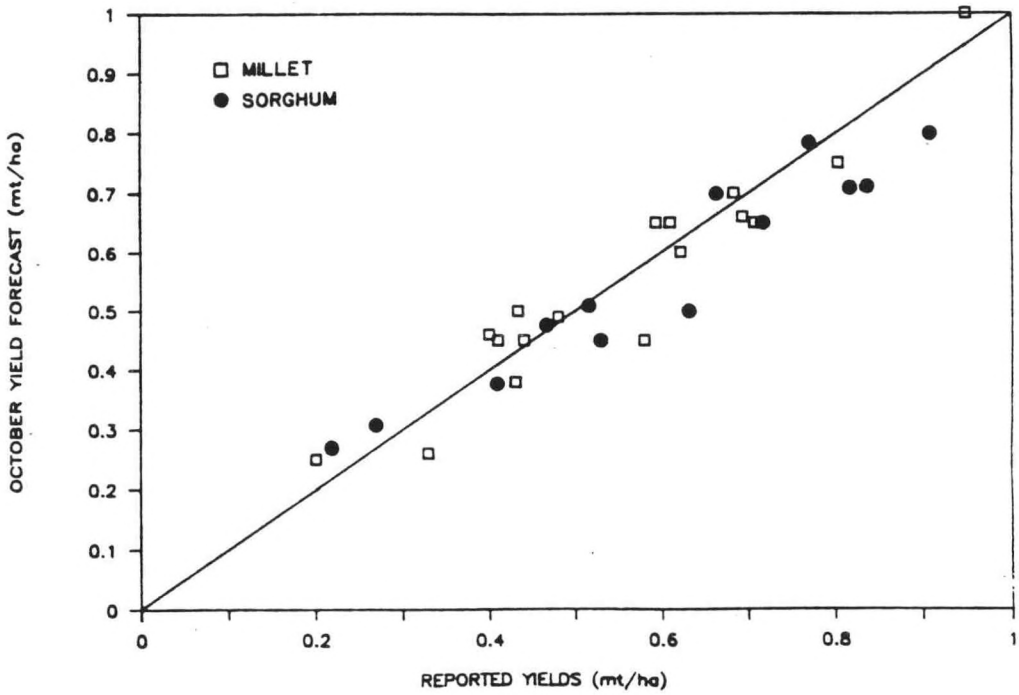

FIGURE 31. Comparison of NOAA/AISC October 1986 millet and sorghum yield forecasts with reported yields for the administrative regions of Niger and Burkina Faso. The diagonal line represents a perfect one-to-one fit between reported and forecasted yields.

TABLE 7. Mean reported yields and departures of forecasted yields for the administrative regions of Niger and Burkina Faso. Reported yields were issued after completion of the Sep. - Nov. harvests.

	Millet			Sorghum		
Forecast Month	Reported Yield (mt/ha)	Departure (mt/ha)	Percent Departure	Reported Yield (mt/ha)	Departure (mt/ha)	Percent Departure
Sept. 85	.59	0.12	20	.62	0.10	17
Oct. 85	.59	0.11	18	.62	0.11	18
Sept. 86	.55	0.06	12	.65	0.07	11
Oct. 86	.55	0.05	9	.65	0.06	10

Because of the uncertainties in the yield data for the Sahel countries, an accurate verification of yield forecasts is not now possible. Nevertheless, the comparison between reported data and forecasted yield in Niger and Burkina Faso, especially for 1986, is encouraging (Kaylen and Le Duc, 1988). These preliminary results suggest that yield estimates at the sub-country level in the Sahel may be obtained as early as the beginning of September.

Although the quantitative yield data may not be reliable in some African countries, subjective field reports from within the respective countries during the course of the growing season can be extremely useful by supplying on-site observations of weather and crop conditions, provided the observations are made by competent and conscientious personnel. If such is the case, the on-site observations should supersede information from other sources. On the other hand, erroneous reports would be very misleading, and worse than no information at all. This potential dilemma underscores the subjective nature of the assessment process. Only as quantitative methods are refined and improved can assessments become more objective and more accurate.

PART IV: SUMMARY AND RECOMMENDATIONS

By early September, analysts are usually able to make reasonably accurate projections of grain yields for harvests to be completed in November. Both qualitative and quantitative assessments of crop conditions in the Sahel countries of Africa appear to be useful for indicating weather-related problems which have the potential to cause food shortages. At the present time lack of reliable historical crop yield statistics makes verification of yield forecasts indeterminate. Nevertheless, preliminary verification efforts suggest that rainfall information, combined with satellite-derived vegetation data, can provide rain-fed crop yield estimates which are quite adequate for emergency food planning.

Because the relationship between yield and rainfall is nearly linear for the range of rainfall usually experienced in the Sahel countries, simple regression models based on monthly rainfall data appear to provide excellent indications of final crop yields in this region. For those areas where rainfall data are not available, models based on the satellite Normalized Vegetation Index at the crop's heading stage appear to offer considerable potential for yield prediction. This is because the NVI results from direct satellite observation of vegetation, integrating weather conditions during the course of the growing season. These models should be used to supplement the rainfall models even in areas with reliable rainfall data.

In Ethiopia, sharp gradients in terrain and climate, lack of a dense network of reporting weather stations, and questionable historical crop data combine to make formulation of quantitative models extremely difficult. However, careful analysis of vegetation imagery and indices, Meteosat cloud imagery, and available rainfall reports has enabled analysts to delineate areas of probable crop failure, most recently in northern Ethiopia during the summer of 1987. This information, evaluated from the perspective of historical weather and vegetation data, along with knowledge of agricultural practices, can be sufficient to categorize the severity of drought and the resulting food shortages.

Future crop monitoring methodology should expand upon the promising tools developed for the African assessments. Other configurations of satellite vegetation indices, such as the Vegetation Condition Index (Kogan, 1987), should be explored. The use of the water balance or FAO index for forecasting crop yields needs to be investigated. The rainfall yield models should be updated as better crop statistics are obtained, and use of 10-day rainfall totals should be considered. Since rainfall data are critical to crop assessments in semi-arid areas of Africa, every effort needs to be made to improve the quality and coverage of rainfall reports and estimates. Digital Meteosat data would streamline input of cloud data for use in satellite rainfall estimation schemes in Africa, and resulting estimates should be automatically merged with reported rainfall totals,

using weighting schemes which reflect the accuracy of the reports as well as their location.

After the severe droughts of 1972-73 and 1983-84 in the African Sahel countries, Sudan and Ethiopia, one viewpoint often expressed was that earlier warning of the magnitude of the resulting food shortages could have saved many more lives through expedited delivery of food aid. Today, with the assessment tools developed by analysts in recent years, especially advances in the effective use of remote sensing data from weather and environmental satellites, it is increasingly unlikely that future drought-induced food shortages will escape early detection.

REFERENCES

Ambroziak, R.A., 1986: Real Time Crop Assessment Using Color Theory and Satellite Data. Ph.D. Thesis, University of Delaware, 211 pp.

Ambroziak, R.A., 1984: A new method for incorporating meteorological satellite data into global crop monitoring. Proc. 18th Int. Symp. on Remote Sensing of the Environment, Paris, France.

American Society of Photogrammetry, 1975: Manual of Remote Sensing, Falls Church, VA.

Arkin, P.S., and B.N. Meisner, 1987: The relationship between large-scale convective rainfall and cold cloud over the Western Hemisphere during 1982-84. MWR, 115, 51-74.

Austin, P.M., 1987: Relation between measured radar reflectivity and surface rainfall. MWR, 115, 1053-1070.

Barrett, E.C., 1970: The estimation of monthly rainfall from satellite data. MWR, 98, 322-327.

Callis, S.L., and D.M. Le Comte, 1987: Operational use of satellite imagery to estimate rainfall in the Sahelian countries of Africa. Preprints, 18th Conf. on Agricultural and Forest Meteorology, W. Lafayette, Amer. Meteor. Soc., Boston, MA.

Cocheme, J. and P. Franquin, 1967: An agroclimatology survey of a semiarid area in Africa south of the Sahara. Technical Note No. 86, WMO, Geneva, 136 pp.

Doorenbos, J., and W.O. Pruitt, 1977: Guidelines for predicting crop water requirements. FAO Irrigation and Drainage Paper No. 24, FAO, Rome, 144 pp.

Food and Agriculture Organization, 1986: Early Agrometeorological Crop Yield Assessment. Plant Production and Protection Paper No. 73, FAO, Rome.

Follansbee, W.A., 1973: Estimation of average daily rainfall from satellite cloud photographs. NOAA Technical Memorandum, NESS 44, Washington, DC, U.S. Department of Commerce, 30 pp.

Frere, M., and G.F. Popov, 1979: Agrometeorological crop monitoring and forecasting. FAO, Rome.

Garcia, O., 1981: A comparison of two satellite rainfall estimates for GATE. J. of Appl. Meteor., 20, 430-438.

Gray, T.T., and D.G. McCrary, 1981: The environmental vegetative

index: the tool potentially useful for arid land management. Proc. 5th Conf. on Biometeorology, Anaheim, CA, p. 205.

Griffith, C.G., W.L. Woodley, S. Browner, J. Teijeiro, M. Maier, D.W. Martin, J. Stout, and D.N. Sikdar, 1976: Rainfall estimation from geosynchronous satellite imagery during daylight hours. NOAA Technical Report ERL-WMPO 7, Boulder, CO, U.S. Department of Commerce, 106 pp.

Gruber, A., and A.F. Krueger, 1984: The status of the NOAA outgoing longwave radiation data set. Bull. Amer. Meteor. Soc., 65, 958-962.

Hielkema, J.U., S.D. Prince, and W.L. Astle, 1986: Rainfall and vegetation monitoring in the Savanna Zone of the Democratic Republic of Sudan using the NOAA Advanced Very High Resolution Radiometer. Int. J. Remote Sensing, 7, 1499-1514.

Holben, B.N., 1986: Characteristics of maximum-value composite images from temporal AVHRR data. Int. J. Remote Sensing, 7, 1417-1434.

Johnson, G.E., A. van Dijk, and C.M. Sakamoto, 1987: The use of AVHRR data in operational assessments in Africa. Geocarto Int., 1, 41-60.

Kaylen, A.M., (Climatic Applications Branch, NOAA, U.S. DOC, Columbia MO 65201) 1986: The formulation of yield/precipitation regression models for the 1986 growing season in the Sahel, 13 pp. (unpublished manuscript).

Kaylen, A.M., and S. Le Duc, (Climatic Applications Branch, NOAA, U.S. DOC, Columbia, MO 65201) 1988: Yield forecasts: recent experience in the Sahel, 32 pp. (unpublished manuscript).

Kidwell, K.B., 1986: NOAA Polar Orbiter Data (Tiros-N, NOAA-6, NOAA-7, NOAA-8, NOAA-9, NOAA-10) User's Guide. NOAA, Washington, D.C.

Kogan, F.N., 1987: Vegetation index for areal analysis of NDVI to monitor crop conditions. Preprints, 18th Conf. on Agricultural and Forest Meteorology, W. Lafayette, Amer. Meteor. Soc., Boston, MA, p. 103.

Milford, J.R., and G. Dugdale, 1986: Rainfall mapping over Sudan in 1986. (Department of Meteorology, University of Reading, England.) Report to the Overseas Development Administration on Research Scheme R 3636.

Motell, C.E., and B.C. Weare, 1987: Estimating tropical Pacific rainfall using digital satellite data. J. Climate and Appl. Meteor., 26, 1436-1446.

Penman, H.L., 1948: Natural evaporation from open water, bare soil and grass. Royal Soc., London Proc. Ser. A, 193, 120-146.

Prince, S.D., and C.J. Tucker, 1986: Satellite remote sensing of rangelands in Botswana. Int. J. Remote Sensing, 7, 1555-1571.

Sakamoto, C.M, and L.T. Steyaert, 1987: International Drought Early Warning Program of NOAA/NESDIS/AISC. In Planning for Drought: Towards a Reduction of Societal Vulnerability, Wilhite, D.A. and W.E. Easterling, Eds., Westview Press, Boulder, CO.

Schneider, S.R., S.R. McGinnis, and J.A. Galtin, 1981: Use of NOAA/AVHRR visible and near-infrared data for land remote sensing. NOAA Technical Report, NESS 84, U.S. Department of Commerce, Washington, DC.

Tarpley, J.P., S.R. Schneider, and R.L. Money, 1984: Global vegetation indices from NOAA-7 meteorological satellite. J. Climate and Appl. Meteor., 23, 491-494.

Thomas, A.R., and V.L. Patterson, 1983: A reliable method for estimating precipitation amounts. Preprints, 5th Symp. on Meteorological Observation and Instruments, Toronto, WMO/AME/CMOS, p. 554.

Todorov, A.V., L.T. Steyaert, and V.R. Achutuni, 1983: Agroclimatic conditions and assessment methods for drought/food shortages in the Horn of Africa. NOAA/AID PASA Document BOF-0999-P-CC-2042-00, U.S. Department of Commerce, 89 pp.

Todorov, A., 1985: Sahel: the changing rainfall regime and the "normals" used for its assessment. J. Climate and Appl. Meteor., 24, 97-107.

Tucker, C.J., J. Gatlin, S.R. Schneider, and M.A. Kuchinos, 1982: Monitoring large scale vegetation dynamics in the Nile delta and river valley from NOAA AVHRR data. Proc., Conf. on Remote Sensing of Arid and Semi-Arid Lands, Cairo, Egypt, p. 973.

Tucker, C.J., C. vanPraet, E. Boerwinkel, and A. Gaston, 1983: Satellite remote sensing of total dry matter production in Senegalese Sahel. Remote Sensing of the Environment, 13, 461-474.

Turpeinen, O.M., A. Abidi, and W. Belhouane, 1987: Determination of rainfall with the ESOC Precipitation Index. MWR, 115, 2699-2706.

van Chi-Bonnardel, Regine, Ed., 1973: The Atlas of Africa. Editions Jeune Afrique, Paris, 355 pp.

van Dijk, A., 1986: A crop condition and crop yield estimation method based on NOAA/AVHRR satellite data. Ph.D. Thesis, University of Missouri, 203 pp.

van Dijk, A., S.L. Callis, C.M. Sakamoto, and W.L. Decker, 1987: Vegetation Index Profiles: an alternative method for reducing radiometric disturbance in NOAA AVHRR data. Photogrammetric Engineering and Remote Sensing, 53, 1059-1067.

AISC 8 A Model for the Simulation of Larval Drift. David F. Johnson, March 1987.

AISC 9 Selective Retrieval of Spectral MRF Model Winds for Marine Applications. Peter J. Pytlowany, March 1987.

AISC 10 A Sectorized Stretched Gridmesh for Modeling San Francisco Bay and Shelf Circulation. Kurt W. Hess, April 1987.

AISC 11 Predicted Winds for Chesapeake Bay from LFM and Observational Data. Kurt W. Hess and Peter J. Pytlowany, August 1987.

AISC 12 Techniques for Estimating Dollar Impacts from Marine Recreational Activity. Isobel C. Sheifer, December 1987.